RECONSTRUCTING PAST STORMINESS IN HALIFAX HARBOUR THROUGH GRAIN-SIZE ANALYSIS OF MARINE SEDIMENT CORES

ERIN WILSON

Supervisor: Stephanie Kienast (Dalhousie University)
stephanie.kienast@dal.ca

A thesis submitted to the
Department of Environmental Science
Dalhousie University
in partial fulfillment of the requirements for the
Bachelor of Science degree with Honours

April 2013

TABLE OF CONTENTS

LIST OF FIGURES

LIST OF TABLES

ABSTRACT

The Intergovernmental Panel on Climate Change (ICPP, Trenberth, 2007) predicts that extra tropical storm tracks will move pole-ward and have higher precipitation rates and larger wind speeds at the end of the 21st century. Because of this, understanding patterns of past storminess in the Atlantic Canadian region has become increasingly important in order to improve the accuracy of modeling and predicting storms in the area. In light of the very short modern instrumental record of storminess in Eastern Canada, 'a long-term proxy based record of storminess, extending back into the Holocene would provide both a basis for the evaluation of trends in past storminess and a firmer foundation for future predictions' (p. 1, Clarke & Rendell 2009) In this study, sediment cores from the Northwest Arm and Purcell's Cove in Halifax Harbour, Nova Scotia were examined for changes in sortable silt (SS) downcore using disaggregated inorganic grain-size (DIGS) analysis. An age model was created using a previously published sedimentation rate estimate in conjunction with existing Mercury (Hg) from one of the cores. Evidence from past studies indicates that grain-size measurements, and specifically SS in marine cores can be used to indicate past storminess on storm-dominated shelves. The results from this study indicate increased storminess in Halifax Harbour during the Little Ice Age (LIA, 1400-1700 CE). Other periods of increased storminess were also visible in the sediment record at ~1835-1885 CE, ~510-910 CE and ~10 CE. Future work should include more dating to increase the accuracy of the age model as well as increased temporal resolution.

ACKNOWLEDGEMENTS

A sincere thank you to Stephanie Kienast for her supervision and all her help with this thesis. A very big thank you also goes to Shannon Sterling for her encouragement and for keeping our whole class on track. Thank you also to Jessica Carrière-Garwood for her help with the Coulter Counter, to John Newgard for the Matlab code, and Paul Hill for putting up with the sonicator noise all summer. Thanks also go out to Mike Parsons and Kate Jarrett at BIO for their help with sample collection. And lastly a big thanks to Al and Chris for all of their editing help and support through this whole process.

CHAPTER 1 - INTRODUCTION

1.1 INTRODUCTION

Understanding the past ocean-atmosphere system is necessary to more fully comprehend how the Earth's climate system works. Building upon this knowledge allows for more accurate models and thus, better predictions of future conditions to be made. Information stored in marine sediments, such as chemical tracers, microfossils and grain-size, is commonly used to reconstruct past environmental conditions. This thesis examines grain-size changes in marine sediment cores from Halifax Harbour, Nova Scotia in an attempt to extend the modern instrumental record of storm activity off Eastern Canada back in time.

1.2 BACKGROUND CONTEXT AND DEFINITIONS

The use of so-called "proxies" is essential to study conditions on Earth before instrumental record keeping began. A proxy is a quantifiable parameter that serves as an indirect measure of past conditions that cannot be measured directly. There are many different types of proxies used to reconstruct different variables. For example, tree rings are used as a proxy for temperature and precipitation, as tree growth is limited by these factors (Fritts et al., 1980). Air bubbles trapped in ice record past atmospheric composition, for example with respect to the greenhouse gases carbon dioxide (CO_2) and methane (CH_4). Temperature at the ice core site can be inferred using deuterium isotopes (Jouzel et al., 2003) and solar variability can be inferred from nitrate concentrations of the ice itself (Traversi et al., 2012).

In addition to tree rings and ice cores, marine sediments are a valuable geologic archive for the reconstruction of past ocean and atmospheric conditions because they often offer undisturbed and continuous geological sequences and can be dated with depth. For example, the isotopic composition of oxygen and carbon in foraminiferal shells is used as a proxy for ice volume (Hays, 1991) and water mass distribution, respectively, in the ocean (Henderson, 2002).

The size distribution, weight percentage or mean size, of terrigenous (i.e. non-biogenic) particles in marine sediments is used as a proxy for bottom current speeds at the time of deposition. Increasing current velocities transport increasingly larger grain sizes (McCave, 1985). For example, the speed of the deep currents in the North Atlantic, which are related to the strength of the North Atlantic Meridional Overturning Circulation (AMOC), has an effect on the grain-size distribution of modern bottom sediments where larger grain-sizes are found in sediments correlating to periods of stronger AMOC (McCave et al., 1995b). Grain sizes are classified into different categories. The study of marine sediments focuses on the fine sand (63-125 μm) to sortable silt (10-63 μm) range. Silts smaller than 10 μm and clays (<3.9 μm) are not used because they act cohesively and do not respond as single particle to hydrodynamic forcing (Ledbetter, 1986; McCave et al., 1995b; McCave & Hall, 2006). The sortable silt (SS) range can be measured through disaggregated inorganic grain-size (DIGS), which looks at the inorganic component of the sediment and assesses individual grains that have not been compacted or crushed.

In shallow ocean conditions, close to the shore, energetic effects of surface waves caused by storms and winds can reach the sea floor. Large storms, such as hurricanes and nor'easters, have been observed to cause localized re-suspension of previously deposited sediments (DeIure, 1983). These sediments can then be re-deposited locally or be carried to other locations near by. For example, sandy sediments can be carried to areas with mud floors on the Scotian Shelf during storm events (Kontopoulos & Piper, 1982).

There are periods in Earth's history that are thought to have had increased storm activity on certain parts of the globe. Strong evidence from multiple studies in Europe show increased storminess during the Little Ice Age (LIA), which lasted from 1400-1700 CE (Hansom & Hall, 2009; Sorrel et al., 2009; Wheeler et al., 2010). These changes could be related to past changes in the North Atlantic Oscillation (NAO), a planetary-scale pattern of climate variability that controls average temperature and precipitation in North America, Europe and Russia. The NAO is known to influence the strength and direction of winds as well as storm tracks across the North Atlantic (Thompson & Wallace, 2001). Changes in storms tracks affect how many storms can reach the Atlantic Canadian region. Oscillations in the NAO may have an effect on periods of increased storminess in the past and in the future. When the NAO is in its low index condition, the subpolar westerlies are weaker, central Europe experiences colder winters, and Nor'easters along the coasts of New England and Atlantic Canada are more frequent (Thompson & Wallace, 2001). There is some modeling evidence that the NAO was in its low index condition during the LIA (Shindell et al., 2001; Mann et al., 2009); however, the exact nature of

the connection between the NAO and storminess on a local to regional scale remains unclear.

1.3 KNOWLEDGE GAPS

A study carried out in Halifax Harbour examined whether large weather events have an effect on sediments closer to shore by looking at modern movement of bottom sediments during wind events and percent sand content in one core. It was concluded that influx of sand to the inner harbour due to coastal transport processes occur during large storm events (DeIure, 1983). This conclusion coincides with evidence of suspended sediment increases during storm events in fjords on the east coast of Canada (Piper et al., 1983; Kontopulos & Piper, 1982).

The modern instrumental record for storm activity off Atlantic Canada does not extend very far back in time. Temperature and precipitation records for Halifax have only been kept since 1871 and wind only began being systematically recorded in 1955 (DeIure, 1983). Other studies (DeIure, 1983; Campbell, 1999) have started to look at using grain-size changes in marine sediment cores as an indicator of past storminess. However, Campbell (1999) looked at cores farther off shore and indicated the need for more sites to be examined on the inner shelf. DeIure (1983) only examined one short core that dated back to 1650. In both studies, the age models were preliminary. In order to test the validity of this approach for constructing a record of past storminess in the area, more sites need to be assessed looking at grain-size change downcore in relation to storm events. This thesis will examine more sites in hopes of further confirming the validity of a grain-size

approach for determining past storminess on a storm-dominated shelf. In addition, it will aid in filling the knowledge gap on storm activity in Atlantic Canada beyond the modern instrumental record.

1.4 GOALS OF THIS STUDY

This study is an extension of the M.Sc thesis on the effect of storms on sediments in Halifax Harbour, Nova Scotia by DeIure (1983). It will look farther back into the sediment record and verify whether or not grain-size measurement can be a valid parameter to indicate past stormy periods. The two objectives of this study are 1) to measure disaggregated inorganic grain-size (DIGS) with depth in two cores and 2) to evaluate whether the sediment cores are suitable for radiocarbon dating

This study will attempt to answer the following questions:

1) How does the grain-size composition change downcore in two cores located in Halifax Harbour (Fig. 1) and how does it compare with modern surface sediments?
2) Can changes in mean or maximum grain-size with depth be correlated to the Little Ice Age (LIA) period ca. 1400-1700 CE?

Overall, the findings of this study will help to determine whether changes in grain-size composition in marine sediments can be used to extend the record of storm activity off Eastern Canada beyond the modern instrumental record.

1.5 SCIENTIFIC IMPLICATIONS

Studying the past is a key aspect of environmental science. By understanding the changes that have happened throughout Earth's history, their causes and their effects, consequences of similar changes and events in the future can be inferred. With climate change towards the end of the 21st century, it is predicted that extra-tropical storm tracks will move poleward and may have larger wind speeds and higher precipitation rates (Trenberth et al., 2007). With the expectation of frequent and stronger storms, the importance of models to predict them becomes increasingly valuable. The more detailed information on past conditions and patterns will lead to the reduction of uncertainty in climate models. With better predictions, mitigation efforts can be focused in the most vulnerable areas.

CHAPTER 2 – LITERATURE REVIEW

2.1 SEARCH METHOD

A formal search method was carried out in order to ensure a comprehensive understanding of the previous research in studying past storminess. Specifically, research on storm-dominated shelves, and the use of grain-size analysis was explored to identify where knowledge gaps exist. The databases used for the search were: GeoRef and Aquatic Sciences and Fisheries Abstracts through Proquest, Web of Knowledge, Science Direct, Oceanic Abstracts through Cambridge Scientific Abstracts and all the Oceanography databases through the "Prowler" search engine at Dalhousie University. For all searches the same keywords were used: marine sediment AND grain-size OR sortable silt AND proxy OR paleo*. In the event that these searches returned too many results, results were narrowed using the keyword storm*. A second search was conducted on the same databases using the keywords: storminess AND North Atlantic OR Eastern Canada OR Little Ice Age. There were no limits set on the searches with respect to the publication date. Methods and theory since research began in this area are fairly consistent with current methods and thought (Inman, 1949; McCave et al., 2006). A focus was put on finding studies that used the sortable silt fraction only; however, when searching sources concerning the reconstruction of past storm events, the search was expanded to allow different types of sediments, such as larger grains, aggregates and terrestrial runoff. These aspects were deemed to be important for understanding the full scope of the field and the variability in techniques based on location and environment. Only English

sources and peer-reviewed research articles were accepted. The only exception to this was one unpublished Masters thesis (DeIure, 1983) and one unpublished Honours thesis (Campbell, 1999) that were not found using the formal search.

2.2 STORM HISTORY IN THE NORTH ATLANTIC

Numerous studies on past storminess in the North Atlantic region focus on storm events; however, nearly all are focused in Europe and little information is available on storminess in Atlantic Canada. In a literature review, Clarke and Rendell (2009) state that instrumental records from both land and sea only date back 200 years and that there are no clear trends in the 19th and 20th centuries. However, a more recent study in Europe (Donat et al., 2011) suggests that storminess has become more intense in the last decades. Archival records such as weather diaries (Golinski, 2001; Nayler, 2006) and lighthouse keeper records (Dawson et al, 2003) date back approximately 800 years and focus on Europe. Records from Royal Navy ships' log books have also been looked at for storm records in the English Channel (Wheeler et al, 2010). However, there is little data collected on storminess in Eastern Canada. Two primary aerosols, marine-source seasalt sodium and continental-source non-seasalt potassium, have been measured in ice cores in Greenland. These records show that winter circulation in the North Atlantic was much stronger during the LIA in comparison to the preceding Medieval Warm Period (MWP, Meeker & Mayewski, 2002).

Consistent with this evidence, coastal dune development in Europe indicates increased storminess during the LIA (Hansom & Hall, 2009). Evidence has also been

found in an estuary in France of less energetic conditions during the MWP and more energetic conditions during the LIA (Sorrel et al, 2009). This evidence of increased storminess in the LIA is supported by human observations from ship logs that noted stronger storms in the English Channel from 1685-1750 CE, one of the coldest periods of the LIA (Wheeler et al, 2010). Trouet et al. (2012) proposed that the cause of increased storminess during the LIA was either a positive or negative state of the NAO. It is still unclear in which state the NAO would have been, as a strong positive NAO is thought to increase storm frequency whereas a strong negative NAO is thought to be linked with increased storm intensity (Trouet et al., 2012).

Most of the current body of research on past storminess in the North Atlantic Region is focused in Europe, and only a few studies on storminess have been carried out in North America. Lake sediments from the Northeastern United States show evidence of increased storminess during the LIA (Noren et al., 2002). Similar to Europe, meteorological data in Eastern Canada has only allowed for modern records of storm events to be documented. These records date back to 1871, with continuous wind records only available since 1955 (DeIure, 1983).

In a review of the literature on future impacts of storms in the North Atlantic, Bader et al. (2011) noted a consensus that there will be a poleward shift of storm tracks; however it is still unclear what the future may hold concerning the number or intensity of those storms. In another review of the literature, Clarke and Rendell (2009) stated that 'a long-term proxy based record of storminess, extending back

into the Holocene would provide both a basis for the evaluation of trends in past storminess and a firmer foundation for future predictions' (p. 1).

2.3 GRAIN-SIZE OF MARINE SEDIMENTS AS A PALEOPROXY

Grain size analysis of marine sediments is used as an indicator of the depositional environment. Deep-sea paleocurrents are studied using the sortable silt fraction of the sediment along with chemical tracers and various dating techniques, for example by McCave et al. (1995b). Many deep-sea paleocurrents studies focus on reconstructing North Atlantic Deep Water (NADW) formation. (Manghetti & McCave, 1995; Hall et al, 1998; Nilsen, 1999; Norgaard-Pedersen & Mikkelsen, 2009).

In hopes of better understanding the modern ocean and its variations, these studies illustrate changes in NADW formation strength and changes in the large-scale circulation in the ocean by looking at the effect of changes in current speed on sediment grain-size on the ocean floor. For example, Federici and McManus (2003) noted changes in deep-sea currents and NADW formation strength during an interglacial period thought to be similar to the Holocene. McIntyre and Howe (2009) also noted changes in SS records showing decreased bottom water flow during stadial periods and increased bottom water flow during interstadial periods in the eastern section of the Greenland-Iceland-Scotland ridge. Studies have also investigated variations in the Lower North Atlantic Deep Water (LNADW) formation. A lag was noted between changes occurring to the NADW and the LNADW during glacial to interglacial shifts (Groger et al., 2003a). Evidence was also

found supporting theories of a superconveyor that existed 3.2-2.75 Ma (Groger et al., 2003b).

McCave and Hall (2006) stated that grain-size methods for paleoceanographic purposes can also be applied to both tidal and shallow water marine environments that undergo wave as well as current effects. The seafloor in shallow water environments is affected by storms and thus, storm events should be visible in the composition of sediment cores.

2.4 RECONSTRUCTING PAST STORMINESS

In reconstructions of past depositional environments, the study design depends strongly on the study location and its present natural conditions. In some cases, multi-proxy approaches are much more useful in differentiating among different types of past coastal events such as storms and tsunamis (Ramirez-Herrera et al., 2012). When looking for evidence of past tsunamis, mean grain size is analyzed, as well as macrobiology, heavy minerals and chemical tracers (Chague-Goff et al., 2011). Terrestrial soil records can also be highly useful, as tsunami and storm surge deposits differ in inland reach and frequency (Ramirez-Herrera et al., 2012) as well as in grain-size and fossil content (Dahanayke & Kulasena, 2008). In river dominated areas in monsoon climates, more terrestrial sediment from runoff is present in marine cores. In these areas, continental magnetite layers (Kissel et al., 2010) and distance of the continental sediment component from the coastline has been used to infer monsoon strength (Clemens & Prell, 1990; Ma et al., 2010). Past storms, such as hurricanes, can also be detected in lake sediments. Malaize et al.

(2011) used pyrite-rich mud layers, an indicator of hypoxic or anoxic conditions, and inputs of marine sediment in a near-shore pond in the Carribean to reveal shifts in the ITCZ and therefore reconstruct past hurricane landfalls. Storm related flood events were identified by large inputs of terrigenous material in 13 lakes in the Northeastern United States (Noren et al., 2002).

Lavelle et al. (1978) noted that the tides affect sediment movement, and also observed that increases in mean current speed and suspended particle concentrations occurred during wind events. On the well-sorted sandy shelf off the coast of North Carolina, increased suspended sediment concentrations were detected during hurricane events with a slightly smaller effect on the outer areas of the shelf (Rodolfo et al., 1971). It is important to observe the effects of present day storms on sediments to better understand how past events can be detected in sediment records.

2.5 PAST STORMINESS OFF THE EAST COAST OF CANADA

The shelf off the east coast of Canada is a storm-dominated shelf receiving tropical cyclones, or their remnants, during the summer months and extratropical nor'easters during the winter (Swift et al., 1986). Inlets on the Scotian Shelf are dominated by wave processes and have comparatively low sediment flux, receiving only 5% of Holocene sediment from rivers (Piper et al, 1983). Most of their sediment supply comes from re-working of glacial till or late glacial pro delta deposits (collectively called "relict sediments", Piper et al., 1983). Piper et al. also observed high suspended sediment concentrations in Halifax Inlet after a storm,

strongly suggesting that re-suspension of bottom sediments took place between 20-30 m water depth. Several laminated silty sand beds that occur at 200 m water depth in the muddy Emerald Basin on the Scotian shelf are thought to represent storm deposits carried from the upper continental slope (Kontopulos & Piper, 1982).

One study on storminess, looking at increases in sand content in marine cores was completed on the Scotian Shelf. Campbell (B.Sc, 1999) examined six cores from the Scotian Shelf, one from the Scotian Slope and one from Drowning Basin on the Grand Banks. Based on very limited chronological control, intervals of higher sand content in the cores appear to correspond with the LIA and the early part of the Holocene (5000-6500 YBP). The data from the cores also possibly indicate a period of reduced storminess during the Climactic Optimum (5500-1250 YBP, Campbell, 1999).

Similarly, DeIure (1983) suggested that sandy laminae in the predominantly mud-floored outer Halifax Harbour correspond to storm events and that storm events were more frequent during the LIA. The sand found in the core is thought to have been transported to the core site during large and more infrequent storm events from the area southwest of McNab's Island (Figure 1).

Both Campbell (1999) and DeIure (1983) stressed the need for more comprehensive dating in order to properly use these results as a record of past storminess in the area and recommended that more locations on the inner shelf be studied in the future. Accurate dating is essential to confirm whether or not core

intervals of higher sand content, and presumably increased storminess, do indeed correspond to the LIA in these areas. Once more and better-dated records exist, the record of storms off Nova Scotia can be more confidently extended beyond instrumental observations.

CHAPTER 3 - METHODS

3.1 OVERVIEW OF METHODS

In sediment samples, there is a relationship between skewness, sorting and mean grain size. From these relationships, the depositional environment of a specific sample could be inferred (Inman, 1949). The grain-size range between 10-63 μm ("sortable silt") is studied in deep-sea environments when examining paleocurrents because grains of that size are small enough to be moved by medium strength currents of 5-10 cm/s (Manghetti & McCave, 1995). Grains smaller than 10 μm act cohesively, much like clays, and therefore are not a good indicator for paleocurrents (McCave et al., 1995a). McCave et al. (2006) stated that the sortable silt fraction can also be used to study near-shore dynamics.

This study used sediment samples from cores in Halifax Harbour. Samples were put through a chemical pre-treatment process before undergoing disaggregated inorganic grain-size analysis (DIGS) using a Multisizer III Coulter Counter.

3.2 STUDY AREA

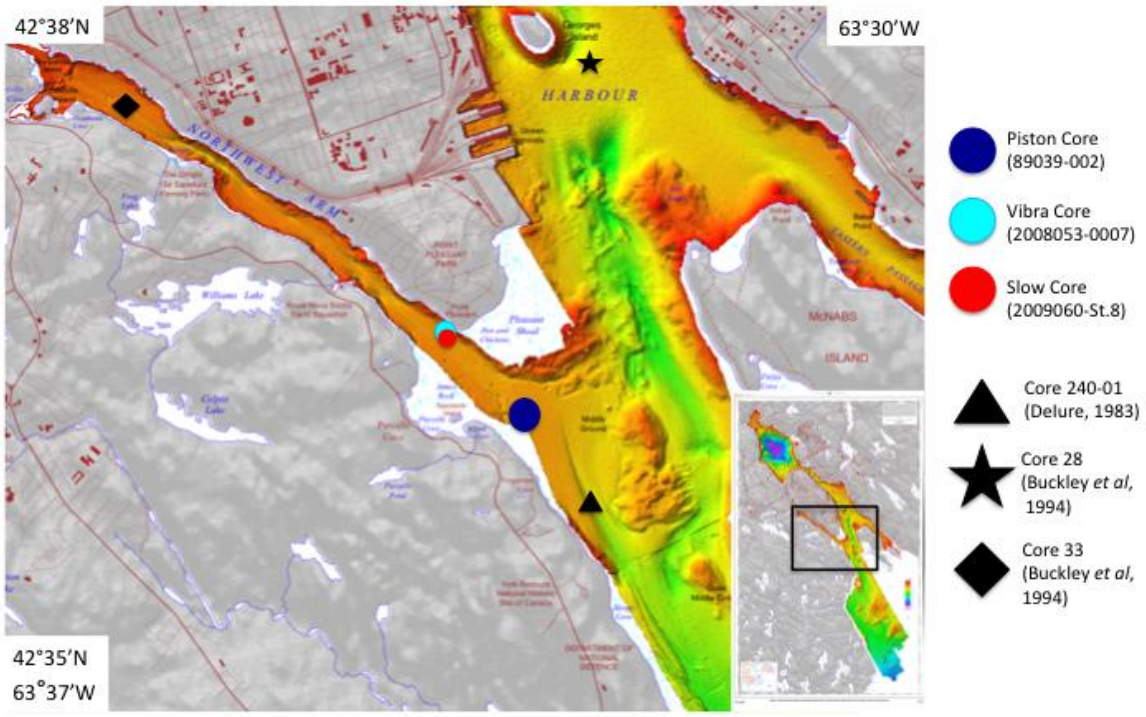

Figure 1: Core locations plotted on a sun-illuminated seabed morphology map. Modified from Figure 6 Fader & Miller (2008). Inset is original map. Black symbols refer to cores mentioned in the discussion. Latitude/longitude values are approximate.

There are two sites located in Halifax Harbour. The first site is located at the mouth of the Northwest Arm and two cores are used from this location, Vibra Core (2008053-0007) and Slow Core (2009060-St. 8). The second site is located further south off Purcell's Cove (Figure 1). Only one Piston Core (89039-002) was used from this location. Detailed information on these cores is provided in Table 1. Like most of Halifax Harbour the seafloor in these locations is mud dominated (Fader & Miller, 2008).

Table 1: Detailed core information

Core Name	2009-060-St. 8	2008-053-0007	89039-002
Alternate Name			89039-3161
Location	Northwest Arm	Northwest Arm	Purcell's Cove
Coordinates Long/Lat (dec.deg.)	-63.5705,44.6172	-63.5710,44.6171	-63.55550, 44.608330
Water Depth	15.5 m	12.5 m	20.1 m
Core Type	Slow Core	Vibra Core	Piston Core
Core Length	35 cm	402 cm	~336cm
Photographs Available		Yes	
Used in Other Studies	Mohamed (PhD., 2013)	Mohamed (PhD., 2013) Williams (MSc., 2010)	
Storage	Refrigerated storage in the National Marine Geoscience Collection of the Geological Survey Canada (Atlantic) at Bedford Institute of Oceanography (BIO)	Refrigerated storage in the National Marine Geoscience Collection of the Geological Survey Canada (Atlantic) at BIO	Ambient storage in the National Marine Geoscience Collection of the Geological Survey Canada (Atlantic) at BIO

The locations were chosen based on core availability and existence of previous work. Williams (2010) used the Vibra Core as well as the Slow Core from the Northwest Arm (among other cores) to study effects of wastewater treatment in the Harbour. From the latter study, mercury and organic carbon concentrations and sedimentation rate estimates, important for dating, were already available. All cores examined here are available at the Bedford Institute of Oceanography (BIO), which allowed for sub-sampling within time and cost constraints of this study.

The sites are located in a busy harbour surrounded by a populated, urban area. However, Fader and Miller (2008) state that most of the disruption of the sea

bed from anchor dragging is caused in the deepest parts of the inner harbour, such as Bedford Basin and the Narrows, not near the study site. Contaminants from the inner harbour also tend to remain trapped in the inner harbour with minimal transport to the outer regions of the harbour (Fader & Miller, 2008). Any significant human effects; however, would only date back about 250 years, when the city was founded and thus, the deeper sediment is expected to be unaffected. For the purposes of this study, it is assumed that 1) sediments at this site have been affected by storm events, 2) man-made scouring of the floor as well as natural erosion is minimal, and 3) input of sediments due to human activities is insignificant.

3.3 CORE COLLECTION

Cores from the Northwest Arm (the Slow Core and the Vibra Core) were collected by Saad A. Mohamed (Ph.D. thesis in preparation, Dalhousie University, 2013). Core 2008053-0007 is a Vibra Core, core 89039-002 is a Piston Core. Both Vibra and Piston coring techniques are used to collect longer cores (up to 20 meters) but these techniques tend to destroy the top layers of the sediment (Tetra Tech, 2003). The Slow core, from the Northwest Arm, on the other hand, retrieved an intact sediment-water interface (Tetra Tech, 2003; Mohamed, 2013).

3.4 SUB-SAMPLING

The Vibra Core and the Piston Core were sub-sampled for this study from intact cores at BIO. Samples of approximately 1 cm^3 were taken using a spatula every 2-5 cm down-core. The intervals that the samples were taken at depended on where the core had been previously sampled for other studies and where enough

material remained. Samples were placed in Whirl-Pak® plastic bags and labeled with core number and depth. Sub-Samples from the Slow Core had already been freeze-dried prior to this sample. Samples were taken every centimeter down-core and were placed in small plastic vials and labeled with core number and depth. Freeze drying does not interfere with DIGS analysis.

Any dateable material, such as shells or twigs, found in the cores was also removed and labeled with the depth at which it was found (Table 2).

3.5 SAMPLE PRE-TREATMENT

The study site is in a coastal area; therefore there is biogenic material in the samples. This material has to be removed through several digestion steps so that the grain-size measured on a Multisizer III Coulter Counter is of the targeted terrestrial, non-organic matter component of the sediments.

Several processes were followed to prepare the samples for grain-size measurement. First, the samples were freeze-dried for three days to remove any moisture and preserve the samples without compacting or crushing the individual particles. Samples from Slow Core did not require this process; as they had already been freeze dried previously. After freeze-drying, a subset of samples was selected for further processing. For the Vibra Core and the Piston Core, samples every 10 cm down-core were used for DIGS analysis and were put through the digestion process. For the Slow Core, samples were run every 2-4 cm.

Sixty mg of sediment for each sample was placed in a test tube. Calcium carbonate and organic matter were removed following the procedure used by McCave et al. (1995a). Four ml of 10% hydrogen peroxide was added to the sample to remove organic matter. The samples were then placed in an ultrasonic bath for 30 minutes. Four ml of 10% hydrochloric acid, used to remove calcium carbonate, was then added and the samples were sonicated for another 30 minutes. Twenty-five ml of nanopure water was added to each test tube and the samples centrifuged for 20 minutes at 400 rpm and decanted. Samples were placed in an oven overnight to dry before biogenic opal was removed using the method in Morlock & Froelich (1989). Fourty ml of 2 M sodium carbonate was added to each test tube. The samples were then placed in a hot bath at 80°C bath for a total time of five hours. After two and four hours, the samples were re-agitated in the ultra sonic bath for five minutes. Samples were rinsed with nanopure water, placed in the centrifuge for 20 minutes at 400 rpm and decanted to remove $NaCO_3$. The last step was repeated three times.

3.6 GRAIN-SIZE ANALYSIS

Grain-size measurements were completed using a Coulter Multisizer III electro resistance particle size analyzer. All of the samples were suspended in an electrolyte solution (1% sodium chloride) made using distilled, ionized water, and were sonicated directly prior to analysis on the Multisizer. DIGS measurements of the electrolyte solution were used as instrument blanks for each aperture tube. Every sample was run using the 30 μm, 200 μm and 400 μm aperture tubes.

Methods were carried out according to the current BIO and Hill Lab at Dalhousie procedures (Appendix I).

The output from the Coulter Counter provides a normalized grain-size distribution for each aperture tube used; therefore, there are three curves for each sample run. These distributions were merged using a Matlab code (Appendix II) to create one normalized distribution for each sample depth. The curves were merged at manually chosen overlapping size bins.

Repeat analysis, using nine separate extractions on the same sample (Vibra Core, 122 cm), was carried out to assess the procedural blank. Lab standard "Sillikers" was also repeatedly run, without pretreatment, as a machine blank. In addition, the grain size composition of marine analytical chemistry standards (HISS-1, PACS-2, MESS-3) was also measured after pre-treatment. Note that the grain-size composition of HISS-1, PACS-2 and MESS-3 is unknown and that a certified reference material for DIGS analysis in marine sediments does not yet exist.

3.7 AGE MODEL

An age model was created in order to be able to date any increases in SS downcore and correlate them with historical events. The age model was established using sedimentation rates and mercury concentration provided by Williams (2010). Mercury levels in Halifax harbour have increased 100-fold since 1900 (Fader & Miller, 2008), so this record was used to estimate which depth in the core corresponds to 100 years ago.

The Piston Core, located in Purcell's Cove, did not have information similar to the Northwest Arm location available. The locations are close in proximity, so the sedimentation rate was extrapolated from the Northwest Arm cores. A more comprehensive dating of this area is needed for future work.

The two cores in the Northwest Arm location were spliced to create a longer record for the site. The Vibra Core lost the top sediment during coring whereas the Slow Core recovered the top sediment layer during coring. There were no Slow Cores available for the Purcell's Cove site, therefore, the top few centimeters of the sediment is assumed to be missing.

Splicing was achieved by comparing the downcore concentrations of Hg and C_{org} in both cores. Mercury concentrations reach a minimum in the Slow Core at 34.5 cm depth of 59 µg/kg. The depth in the Vibra Core that most closely resembles this value is at 21 cm depth with a value of 50 µg/kg. In both cores, Hg concentrations rapidly decline below these depths. It was therefore assumed that 21 cm depth in the Vibra Core is equivalent to 35 cm in the Slow Core, and that the top 14 cm were lost during Vibra coring. Depths in the Vibra Core were therefore corrected by adding 14 cm (i.e. corrected depth = actual depth + 14 cm). The corrected depth reflects the actual depth of the samples in the environment.

The corrected depths based on Hg levels can be double checked by looking at other geochemical properties. Organic Carbon (% dry wt.) values are higher in the Slow Core and decrease with depth. There is a minimum of 2.75 % at 31.5 cm and then a slight increase to 3.19 % at 34.5 cm. This corresponds to a similar value at 21

cm of 3.30 % in the Vibra Core. Although there is a slight difference in the values measured between the two cores, the measurements are close and do support the splicing described above (Figure 2).

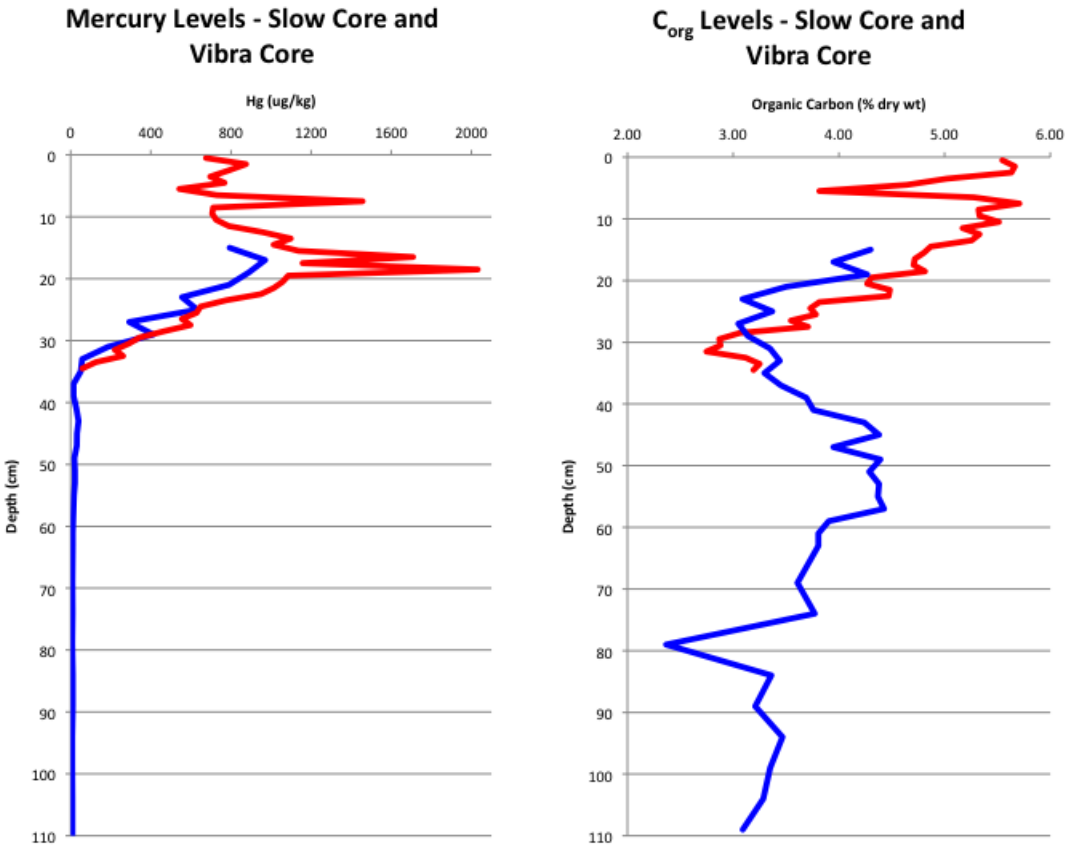

Figure 2: Mercury and Organic Carbon levels vs depth in the Slow Core (red) and Vibra Core (blue). The Vibra Core is plotted with corrected depth (actual depth + 14 cm)

Once all of the data was collected and graphed the following metrics were calculated:

Table 2: Description of Metrics Calculated

Metric	*Description*
Sortable Silt (SS)	Mean grain-size in the 10-63 μm range of the sample
Clay/Silt Ratio	Ratio of the 1-4 μm range to the 4-63 μm range
Cohesive/Non-Cohesive Ratio	Ratio of the 1-10 μm range to the 10-63 μm range
1-8/8-63 Ratio	Ratio of the 1-8 μm range to the 8-63 μm range
Maximum Grain Size	The largest grain size recorded in each sample

CHAPTER 4 – RESULTS

4.1 NORTHWEST ARM

4.1.1 Sortable Silt

Sortable Silt (SS) at the Northwest Arm site ranges from 15 to 27 μm. There is a large variability within the top 35 cm of the record (Figure 3), with maximum values of 27, 25 and 25 μm at 0.5, 8.5 and 10.5 cm respectively. Within this top section there are also minima of 16.5 and 15.1 μm at 4.5 and 22.5 cm depth. Below 30 cm depth, there are still significant variations, but the maximum values do not exceed 21 μm. Single peaks in sortable silt occur at 87 cm and 128 cm. There is also a significant increase between 228 cm and 298 cm depth (Figure 3). Values begin to increase again at the bottom of the core below 378 cm.

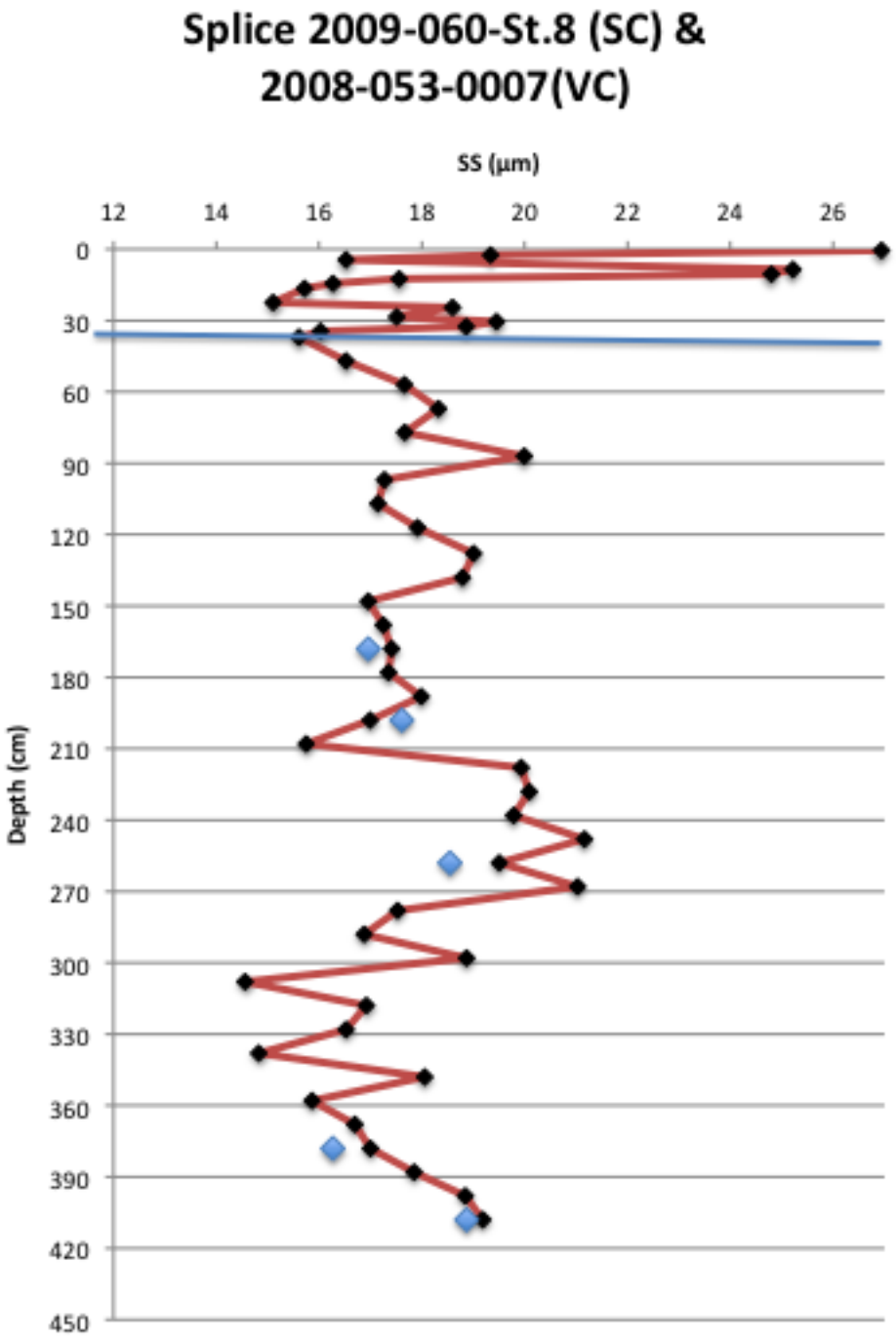

Figure 3: Sortable Silt versus depth (corrected) in the spliced record from the Northwest Arm. Blue line indicates where the cores were spliced. Blue diamonds show duplicate runs.

4.1.2 Other Parameters

Other parameters, the silt/clay ratio, the 1-8 μm/8-64 μm ratio, the cohesive/non-cohesive fraction and the maximum diameter were also assessed. These parameters are only briefly described here, but graphs can be found in Appendix III.

As expected, the trends in the cohesive/non-cohesive ratio are opposite to those in the SS index, with minima in this ratio occurring when SS values are maximal. Again, there is large variability within the top 35 cm, with maximum values of 4.5 and 4.8 μm at 4.5 cm and 22.5 cm and minima of 0.5 and 0.7 at 0.5 cm and 8.5 cm (Figure AIII.2). There is significant variability below 35 cm, but the minimums and maximums do not display the same extremes. Smaller values are noticeable between 67 - 138 cm, between 228 - 298 cm and again at the bottom of the record below 378 cm.

The trends in the 1-8 μm/8-64 μm ratio reflect those seen in the cohesive/non-cohesive ratio. Maxima and minima occur at the same depths. The values are slightly lower and range from 0.44 - 3.7 μm (Figure AIII.3).

The clay/silt ratio also shows similar trends to the cohesive/non-cohesive ratio and the 1-8 μm/8-64 μm ratio. The values are smaller than the other parameters assessed with minimums of 0.3 and 0.25 μm occurring above 10 cm and maximums of 1.2 μm visible at 4.5 cm and 22.5 cm depth (*Fig. AIII.1*).

Maximum diameter was also calculated. This parameter showed large variations from 48.5 μm - 78.5 μm within the top 10 cm of the core (*Fig. AIII.4*).

Maxima correspond to maxima in SS and minima in the other ratios measured. There is much less variability below 10 cm depth with the maximum grain size varying between 42.2 μm and 55.7 μm.

4.2 PURCELL'S COVE

4.2.1 Sortable Silt

SS values at the Purcell's Cove site range in value from 16 - 23 μm downcore (Figure 4). There were larger values (~27 μm) in the upper part of the Northwest Arm record that do not appear in the Purcell's Cove record, consistent with the presumed core top loss at this site. Compared to the Vibra Core of the Northwest Arm record (i.e. below 35 cm), the Purcell's Cove site does show higher values of sortable silt on average.

Larger peaks in SS occur within the top 60 cm of the record, with values of 23 and 22 μm at 23.5 and 54.5 cm depths respectively. There are also SS peaks at 95.5 cm, between 148.5 - 169.5 cm and again near the bottom of the core between 285.5 - 315.5 cm depth. There is also a larger increase visible below 325.5 cm. Minima occur between 64.5 - 84.5 cm, 128.5 - 138.5cm, 179.5 - 202.5 cm and again between 226.5 - 265.5 cm depth.

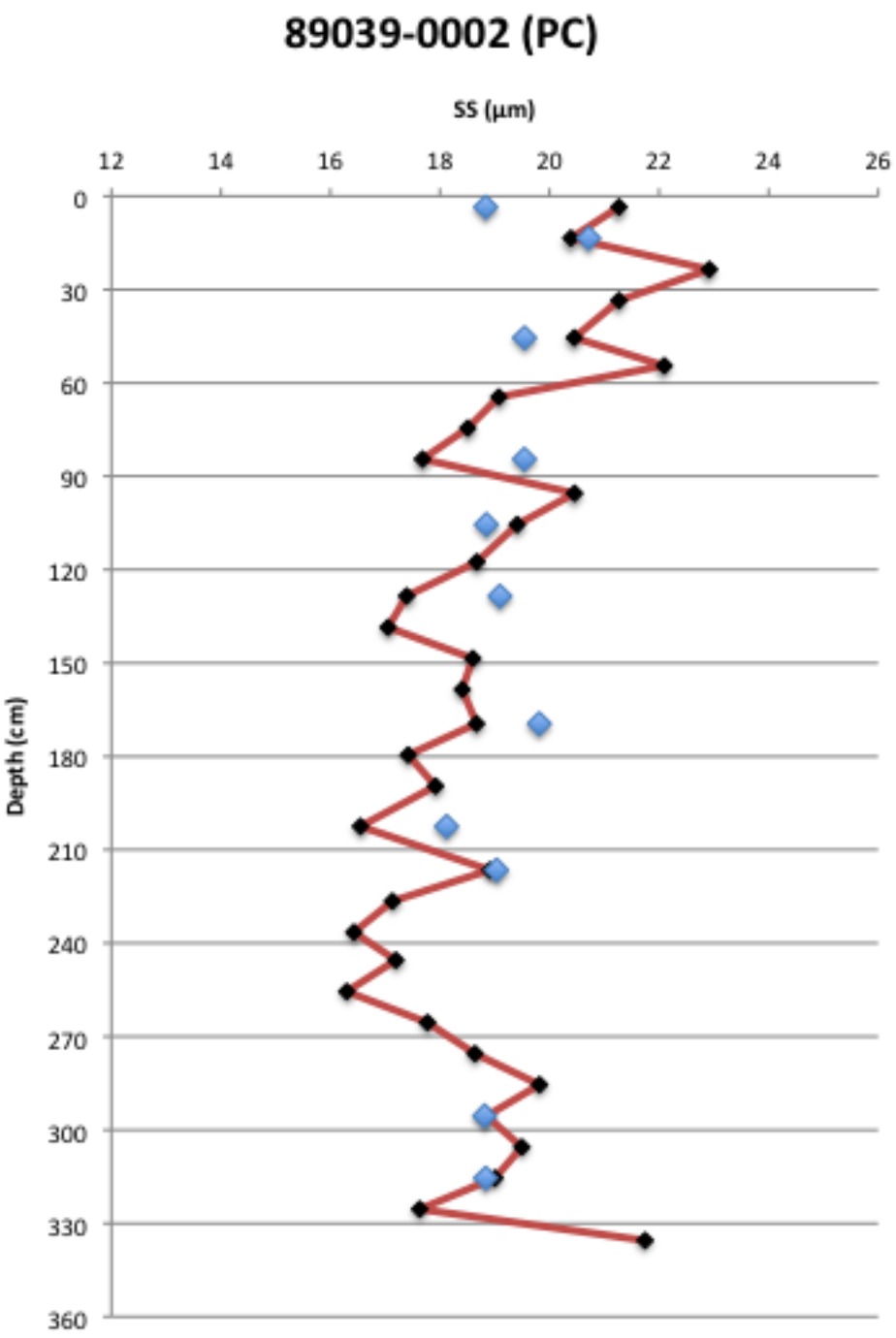

Figure 4: Sortable Silt versus depth in core 89039-0002 from Purcell's Cove. Blue diamonds show duplicate runs.

4.2.2 Other Parameters

Other parameters, the silt/clay ratio, the 1-8 μm/8-64 μm ratio, the cohesive/non-cohesive fraction and the maximum diameter are briefly discussed here. Graphs of these parameters can be found in Appendix III.

As with the Northwest Arm site, the trends in the cohesive/non-cohesive ratio are opposite to those observed in the SS index, with maxima of the cohesive/non-cohesive ratio occurring at depths of minimal SS. The values of the cohesive/non-cohesive ratio range from 0.68 to 3.5 downcore.

The 1-8 μm/8-64 μm ratio values vary from 0.55 - 2.5 downcore with trends similar to those seen in the cohesive/non-cohesive ratio. The clay/silt ratio also follows similar trends with values ranging from 0.24 - 0.76 downcore. These values are larger than those seen at the Northwest Arm site.

The maximum grain size at this site ranged from 42 μm to 73 μm. These values are within the range of the Northwest arm site.

4.3 STANDARDS AND DUPLICATE RUNS

Duplicate runs and standards were assessed in order to determine procedural and instrumental blanks. Sample 122 cm (Vibra Core) was chemically treated and analyzed on the Coulter Counter nine times and its SS value was calculated over the 10-63 μm range (Figure 5). The standard deviation is 1.7 μm, meaning that any changes in SS in the cores must be larger than this to be considered significant. Changes in SS downcore of less than 1.7 could be caused by

a) uncertainties related to the pre-treatment and DIGS measurement or b) natural variability within the individual samples.

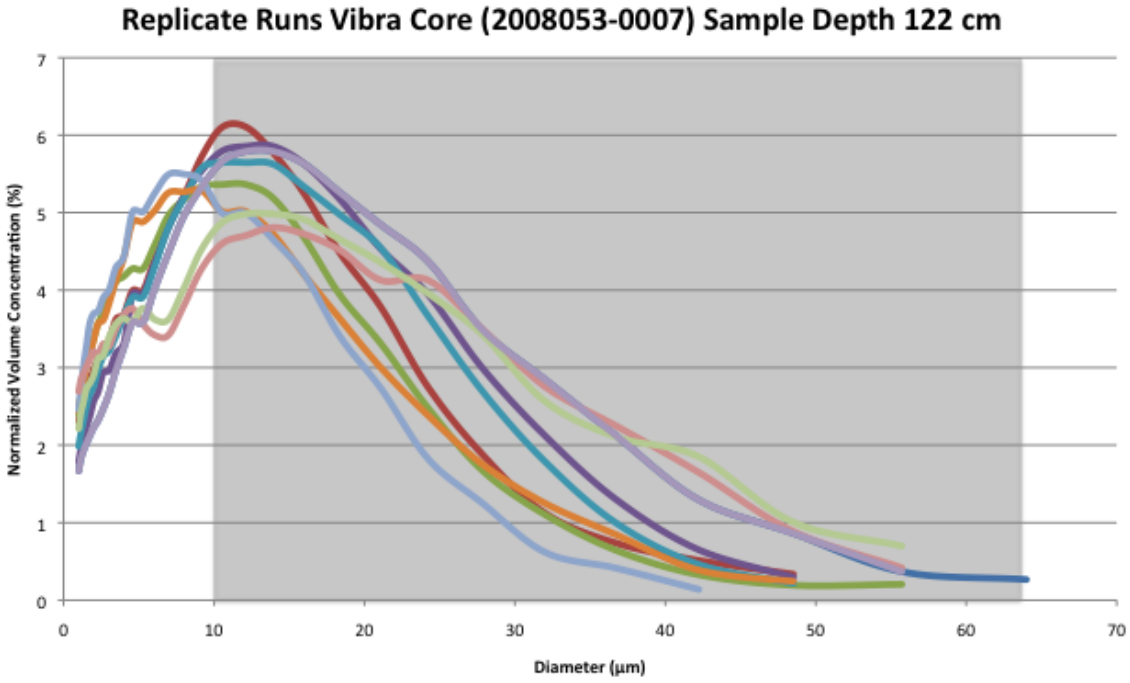

Figure 5: Normalized Grain-size distributions from sample depth 122 cm from the Vibra Core (2008053-0007). SS range is indicated by grey box.

Three certified marine geochemical standards were also tested for grain-size distributions (Figure 6). These standards were chosen here due to a lack of certified grain-size standards for marine sediment. HISS-1, PACS-2 and MESS-3 were run through the entire procedure process and the results are displayed in Figure 6. Standard deviations for SS derived from the measurements are 1.0, 2.1 and 0.3 µm respectively. The "Sillikers", an internal lab standard used in the Hill Lab was run only on the Coulter Counter as a machine blank without pre-treatment. The standard deviation for the Sillikers was 0.2 µm. Additional Sillikers data was kindly provided by Laura DeGelleke *(see* DeGelleke et al. 2013 *for details)*. The standard

deviation calculated for these samples was 0.5 µm. Again, these Sillikers acted as a machine blank had a much lower standard deviation than the pre-treated repeat extractions. The standard deviation of the procedural blanks (122 cm, HISS-1, PACS-2 and MESS-3) is higher than that of the machine blank (Sillikers) due to the added steps of the pre-treatment process and potential natural heterogeneity in the case of sample 122 cm.

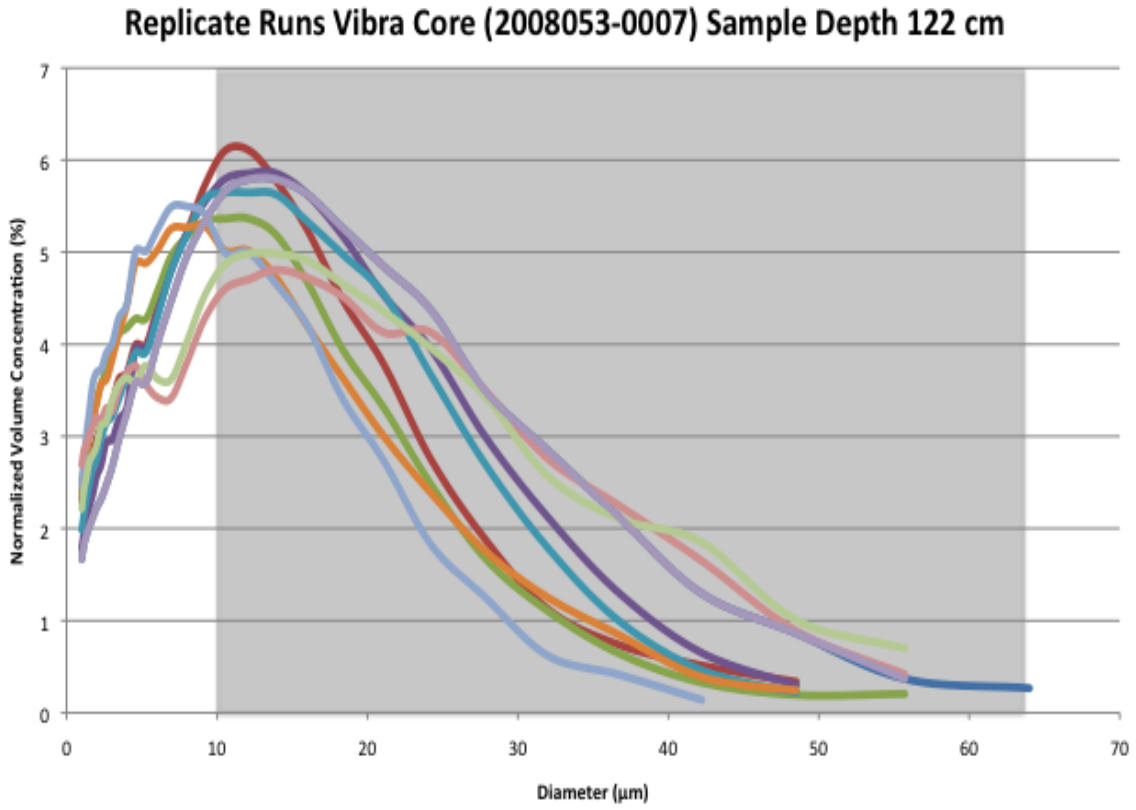

Figure 6: Normalized volume concentration (%) for marine analytical chemistry standards (National Research Council Canada) used for procedural blanks and untreated 'Sillikers' used as a machine blank.

A high variability in the "maximum grain-size" metric is apparent in the replicate runs (*Fig. 5*) as well as in the standards; most notably in the PACS-2 and HISS-1 but also in Sillikers and MESS-3 (Figure 6). This points to the unreliability of

using this metric and is related to the fact that it only takes one coarse particle to significantly skew the volume % distribution in the larger grain-size spectrum.

4.4 MATERIAL FOR C-14 DATING

Material for dating was found in the Vibra Core. There was no datable material found in the other cores. Details are listed in Table 3.

Table 3: Datable organic matter collected in this study

Core #	Location	Depth	Material Found
2008053-0007	Northwest Arm	47.5 cm	Shell fragments
2008053-0007	Northwest Arm	152.5 cm	Twig
2008053-0007	Northwest Arm	227.5 cm	Twig

4.5 AGE MODEL

The sedimentation rate in the Northwest Arm is 0.2 cm/year based on ^{210}Pb measurements carried out by Williams (2010) on the Slow Core. Mercury levels in the Northwest Arm drop significantly to 58 µg/kg at a depth of 19 cm in the Vibra Core (non-adjusted depth) and to 59 µg/kg at a depth of 34.5 cm in the Slow Core (Figure 2).

There are no published sedimentation rate estimates for the Purcell's cove area, but other sedimentation rate estimates in the Northwest Arm (0.15 cm/yr, core 33, Buckley et al, 1994) and near Georges Island (0.65 cm/yr, core 28, Buckley et al, 1994) are within the same order of magnitude (Figure 1). In light of the

available data, and because the Slow Core was the closest with a known sedimentation rate, the same rate (0.2 cm/yr) was used for both sites examined in this study. Also, due to the fact that piston cores are known to over penetrate the top-most layers of sediment, it was assumed here that the top 20 cm is missing. In the absence of any other available age control, constant sedimentation rates were assumed for the entire record. Based on these assumptions, a preliminary age model was established for the Purcell's Cove site and the Northwest Arm site.

4.6 SUMMARY OF RESULTS

All of the grain-size parameters show similar trends down-core. Maximum grain size (refer to section 4.3) is not a good representation of the sediment composition as a whole as the presence or absence of one particle can skew these measurements significantly. All of the ratios described above are different ways to interpret the same data; therefore, the discussion will focus solely on the SS output.

CHAPTER 5 – DISCUSSION

5.1 COMPARISON WITH MODERN SURFACE SEDIMENTS

Modern surface sediments from the Northwest Arm to the south of Purcell's Cove are mainly composed of LaHave Clay, a silty to sandy clay or a sandy to clayey silt with some dropstones and shells (Fader & Miller, 2008). The down-core grain-sizes observed at both sites fall within the silt range and the very lower part of the sand range according to the Wentworth Scale (Wentworth, 1922) and are therefore consistent with modern surface sediment composition.

5.2 DOWNCORE TRENDS

There are notable periods of increased SS values down-core at the Northwest Arm site. Large values are notable within the last 50 years (the top 10 cm). There are other notable peaks between approximately 1835 and 1885 CE (dates are based on years before 2010 CE noted in Figure 7, 25–35 cm) and ~1570 CE (80 cm). A longer period of increased sortable silt is visible between 510 and 910 CE (200-280 cm) and there is another slight increase at the bottom of the core around 10 CE (380 cm, Figure 7).

The Purcell's Cove record does display the high variability at the top, consistent with the assumption of core top loss at this site in comparison to the Northwest Arm site. There is a slight overall decrease in SS down-core. There are peaks that may correspond in time with SS peaks at the Northwest Arm site. For example, the peak at ~1795 CE may correspond to the peak between ~1835-1885

CE described above. There is also a peak at ~1435 CE that may correspond to the peak at ~1570 CE in the Northwest Arm. Another small peak occurs ~830 CE, within the range of the large increase between 510- 910 CE in the Northwest Arm, but it is not as prominent at the Purcell's cove site. This core also displays an increase in SS towards the bottom of the core starting about 410 CE (Figure 8). The age models for the Purcell's Cove site in particular, but also for the Northwest Arm site are preliminary and the conclusions described above are still speculative until more accurate data becomes available.

Overall the sediment composition in Purcell's Cove is slightly coarser than that of the Northwest Arm site. This is consistent with the observations that larger particles are carried into the harbour from further out on the shelf, to the south of the study sites (DeIure, 1983). As Purcell's Cove is south of the Northwest Arm (Figure 1), larger particles would settle out there first.

5.3 UNCERTAINTY OF THE AGE MODEL

The age model is based on a sedimentation rate estimate calculated from Pb-210 measurements in the upper 10 cm of the Slow Core (0.2 cm/yr, Williams, 2010). Since no other age constraints are currently available, this sedimentation rate is extrapolated down-core and assumed to be constant.

The sedimentation found in the Northwest Arm by Williams (2010) was also used for the Purcell's cove site due to a lack of dated cores close by. Due to these factors, there is uncertainty in the age model used, and the uncertainty likely increases down-core as sedimentation rates could have varied over time. The effect

of possible changes in sedimentation rates of the most notable peaks is illustrated in Table 4.

Table 4: Dates of significant peaks with different sedimentation rates

	Sedimentation Rates		
	0.15 cm/yr	**0.2 cm/yr**	**0.25 cm/yr**
Northwest Arm	~1780-1850 CE	~1835-1885 CE	~1872-1912 CE
	~1535 CE	~1570 CE	~1724 CE
	~125-660 CE	~510-910 CE	~880-1200 CE
	~540 BCE	~10 CE	~480 CE
Purcell's Cove	~1720 CE	~1795 CE	~1835 CE
	~1240 CE	~1435 CE	~1550 CE
	~435 CE	~830 CE	~1065 CE

5.4 INTERPRETING SS AS A PROXY

It is well documented that with increased bottom current speeds, coarser and better sorted silts are present on the sea floor (McCave, 1985; Ledbetter 1986). DeIure (1983) noted an increase in the concentration of suspended sediments near the sea floor during storms. From this evidence, this study interprets the larger silts downcore as evidence of past increased bottom current speed and possible sediment redistribution. This study suggests that periods of increased SS values therefore correspond to periods of increased storminess in the study region.

The down-core SS distribution at the Northwest Arm site suggests increased storminess between 1835-1885 CE, ~1570 CE, between 510-910 CE and ~10 CE.

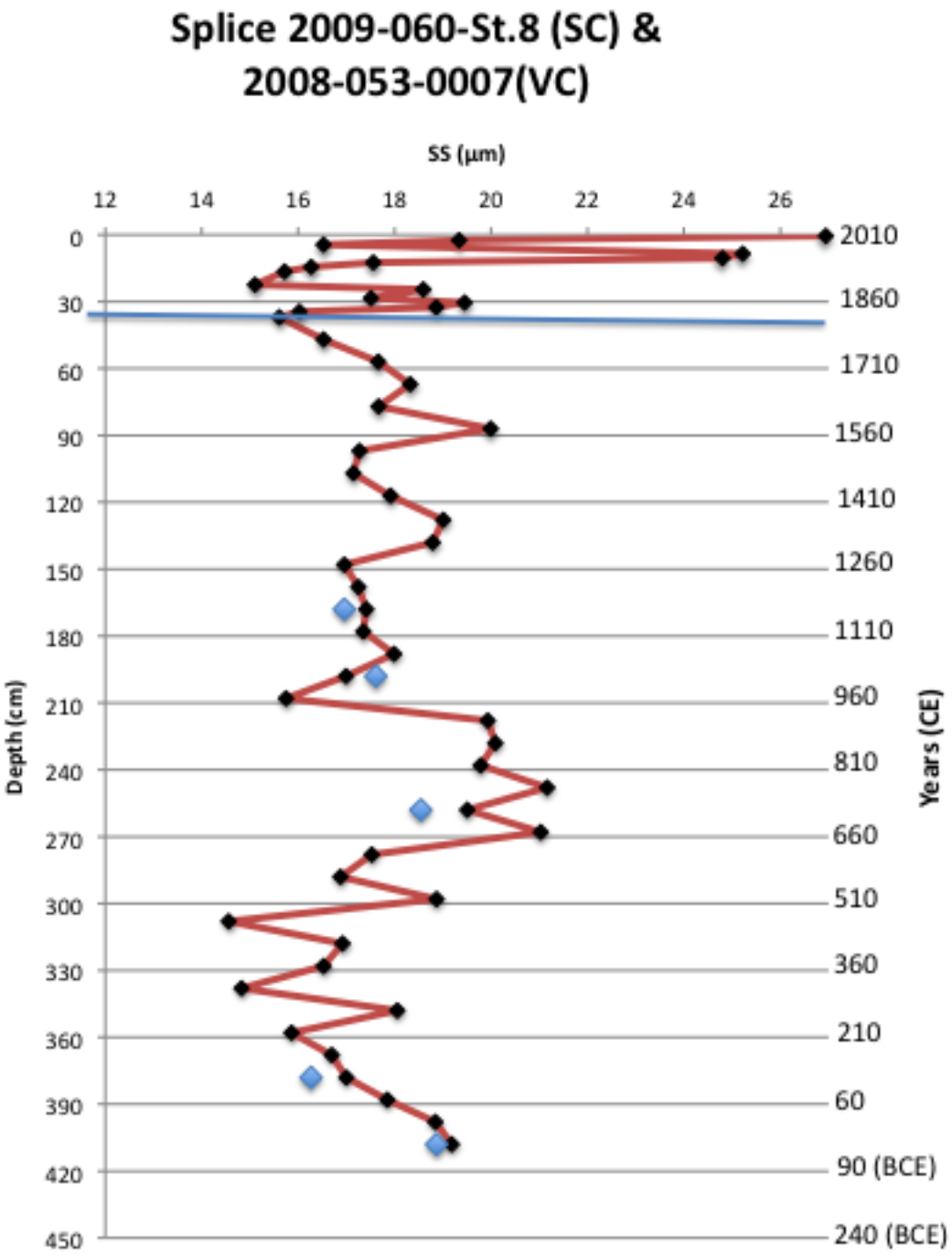

Figure 7: Sortable Silt (SS) distribution versus age and depth (corrected) in splice of core 2009-060-St. 8 and core 2008-053-0007 from the NW arm. Blue line indicates where the cores were spliced. Blue diamonds show duplicate runs.

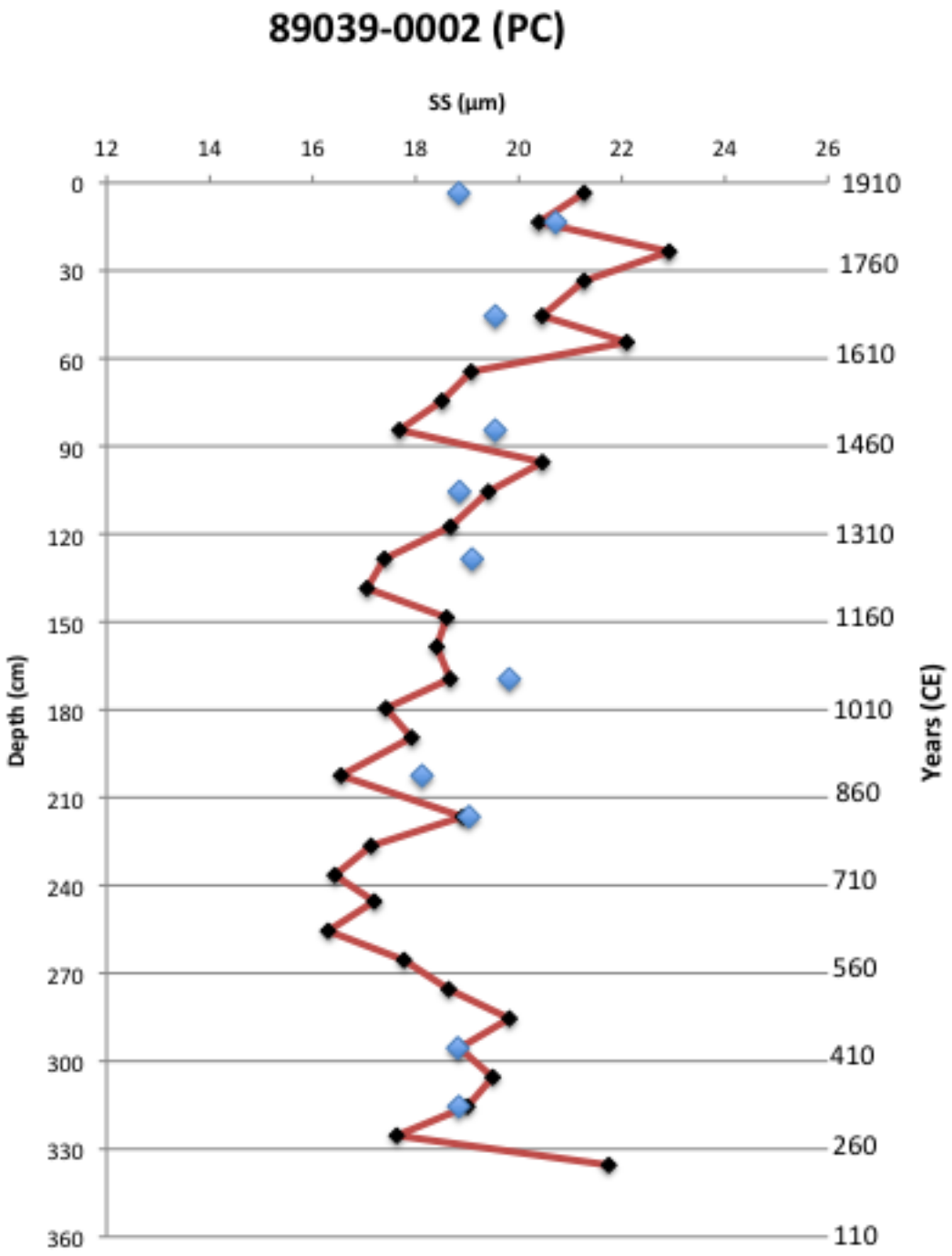

Figure 8: Sortable Silt (SS) distribution versus age and depth in core 89039-0002 from Purcell's Cove. Blue diamonds show duplicate runs.

5.5 STORMINESS IN THE LIA

The LIA lasted from 1400-1700 CE (Wheeler et al., 2010). There is a significant SS peak at ~1570 CE in the Northwest Arm and another peak just outside this time range around ~1360 CE. There are also notable peaks in SS at the Purcell's Cove site at ~1620 CE and ~1420 CE. Acknowledging that the age models derived in this study are still preliminary, these peaks broadly fall into the LIA, and therefore add to the evidence of increased storminess during this time, fitting with the results from Noren (2002) and multiple European studies (Golinski, 2001; Dawson et al, 2003; Nayler, 2006; Hansom, & Hall, 2009; Sorrel et al, 2009; Wheeler et al, 2010)

It is still unknown whether there was an increase in frequency or intensity of storms at this time (Trouet et al, 2012). The evidence of increased SS during this time period does not distinguish between intensity and frequency. However, it can be speculated that the periods of increased SS were caused by an increase in winter storms. The east coast of Canada receives predominantly post-tropical and hurricane storms in the summertime and nor'easters in the winter. Since increased storminess was also seen in Europe at this time (Section 2.2), and Europe is less likely to see strong summer hurricanes, increased storminess during the LIA could possibly indicate a southern movement of the winter storm track in the area. A southward movement of the winter storm track during cooler periods is qualitatively consistent with its predicted northward movement under greenhouse warming at the end of the 21st century (Trenberth *et al*, 2007; Bader *et al*, 2011).

5.6 COMPARISON WITH LOCAL STUDIES

DeIure (1983) examined percent sand in one core from south of Purcell's cove near Furguson's Cove (Figure 1). This parameter is different from SS but still shows indications of increased grain-size down-core. DeIure (1983) correlated two periods of increased storminess from forestry data with the downcore sandy laminae observed near Furguson's Cove. The first of these stormy periods (1800-1860 CE) correlates with increased SS in the Slow Core from the Northwest Arm (Figure 7). The second stormy period she identified correlates with a very slight increase in SS. This increase does fall just within the error calculated and therefore is not a significant increase. The temporal resolution in the DeIure (1983) core (one sample every cm or every 5 years) is much higher than that in the spliced core (one sample every 50 years), and this increase therefore may have been missed.

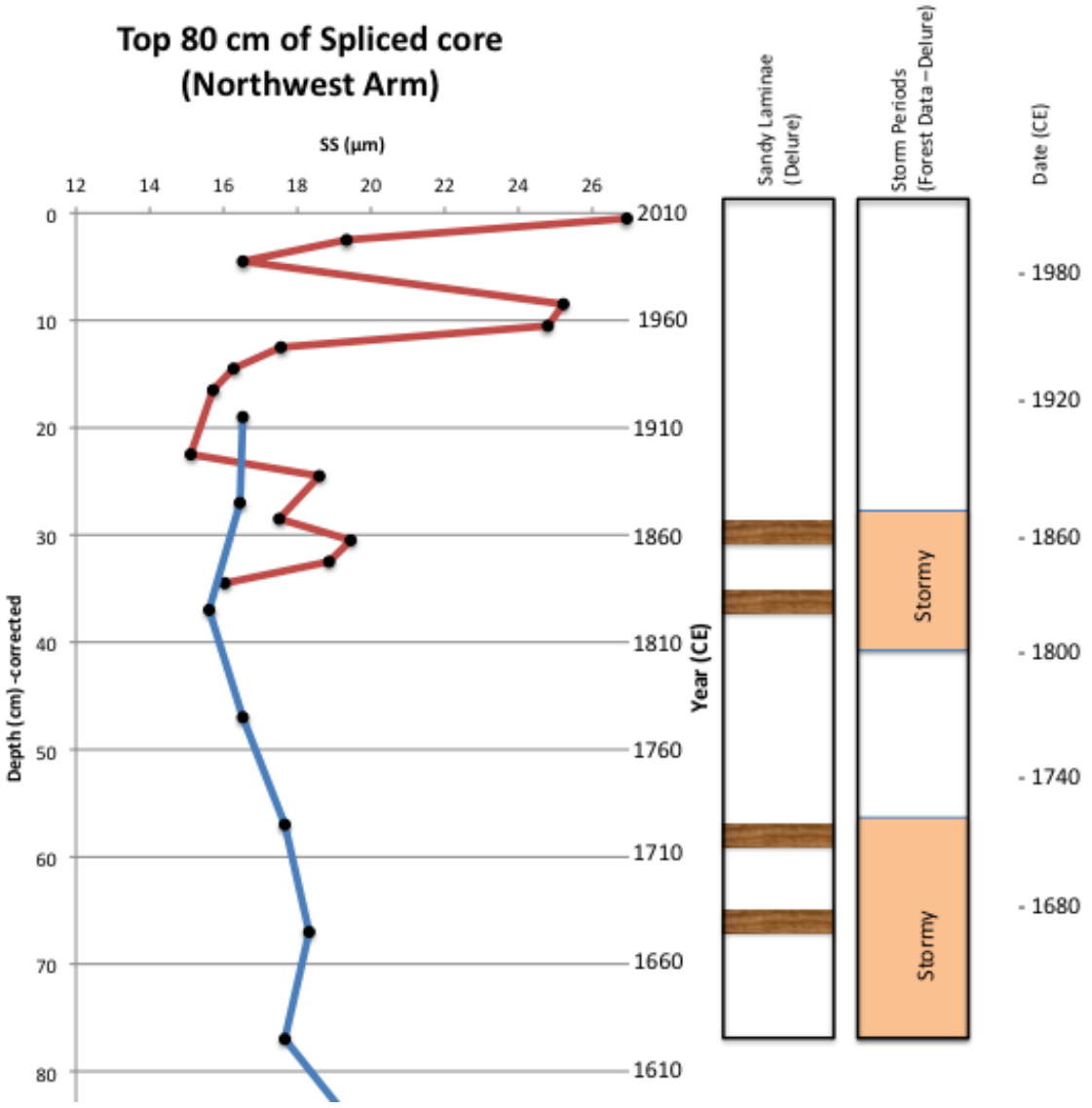

Figure 9: SS data from top 80 cm of spliced record in the Northwest Arm compared to sandy laminae and forestry storm data from DeIure (1983) Figure 3.4

Campbell (1999) also noted possible increased storminess during the LIA. The decrease in SS between 1800-1500 years ago (at 1500 CE in Figure 7) does correspond to observations made by Campbell (1999) that there could have been a period of decreased storminess during the Climactic Optimum (3500 BCE - 750 CE). However, both the Northwest Arm and Purcell's Cove sites show a significant increase in SS after 410 CE and 110 CE respectively (Figure 7 & Figure 8). Similar to

this study, the age models used by Campbell (1999) are preliminary, and the correlations made above must be tested rigorously in future studies.

5.7 RECENT VARIATIONS IN THE SS INDEX

The Slow Core from the Northwest Arm showed very large variations in SS within the top 10 cm, or the last ~50 years. These variations are consistent with recent, large atmospheric disturbances such as Hurricane Juan in 2003 and 'White Juan' in 2004. Storms of a similar intensity in the past may have had a similar effect on surface sediments, but these high amplitude signals would have been dampened overtime by bioturbation and sediment compaction and appear now as the lower amplitude signals down-core.

5.8 RECOMMENDATIONS FOR FUTURE WORK

To ensure the best locations are used for future work with this proxy, new cores should be taken at silt/mud transitions to specifically look at SS. Both Slow Cores and Vibra/Piston Cores should be taken to ensure a continuous record down-core as well as to ensure that the more recent signals are not missed. More work on other storm-dominated shelves would further test the validity of this proxy.

Dating needs to be carried out to increase the accuracy of the age models. Radiocarbon and Pb-210 dating on all cores would be ideal. There is some dateable organic matter available that was collected for this study from the Vibra Core (Table 2).

This study was a pilot study and only measured the grain-size distribution in samples every 10 cm down-core making for a temporal resolution of one sample every ~50 years. However, subsamples of the cores were taken at 2 cm intervals and are available for future assessment. Using these samples, the resolution could be increased to one sample every ~10 years. Further sub-sampling of the cores could be done to achieve an even higher resolution.

There are no certified grain-size standards for marine sediment available. In analogy to the existing certified standard for geochemical studies, a grain-size standard should be developed in order to ensure the accuracy of findings and reliability of analytical instruments across laboratories.

5.9 CONCLUSIONS

One of the cores used in this study is dateable and variations in SS down-core were observed in this study that are broadly consistent with earlier work from 30 years ago. This points to the validity of a grain-size approach for determining past storminess on a storm-dominated shelf. Evidence was found for increased storminess in the Halifax Harbour area during the LIA. Other periods of increased storminess were also visible in the sediment record at ~1835-1885 CE, ~510-910 CE and ~10 CE.

In light of the findings presented here, we suggest that with more comprehensive dating and higher temporal resolution, a record of storm activity off the Atlantic Coast of Canada can be reconstructed that extends well beyond the modern instrumental record. Having such a record is important to hindcasting

climate models and to improving their accuracy. These models could help to further understand the workings of the NAO as well as predict future storm activity in the area. The accuracy of future storm predictions will become more and more socially important as it is predicted that extra-tropical storms will have higher precipitation and larger winds and their tracks will move pole-ward with current climate change (Trenberth, 2007). These models could also become essential in implementing mitigation efforts in the most threatened areas.

References

Bader, J., Mesquita, M., Hodges, K., Keenlyside, S.O., Miles, M. (2011). A review on Northern Hemisphere sea-ice, storminess and the North Atlantic Oscillation: Obervations and projected changes. *Atmospheric Research, 101, 809-834.*

Buckley, D.E., Smith, J.N., Winters, G.V. (1995). Accumulation of contaminant metals in marine sediments of Halifax Harbour, Nova Scotia: Environmental factors and historical records. *Applied Geochemistry, 10, 175-195.*

Campbell, D.C. (1999). *Holocene storminess on the Scotian Shelf; The Last 7000 Years*. (Unpublished Honours Thesis). Saint Mary's University, Halifax, Nova Scotia.

Chague-Goff, C., Schneider, J., Goff, J. R., Dominey-Howes, D., & Strotz, L. (2011). Expanding the proxy toolkit to help identify past events - lessons from the 2004 Indian Ocean tsunami and the 2009 South Pacific tsunami. *Earth-Science Reviews, 107*,1-2,107-122. doi: 10.1016/j.earscirev.2011.03.007

Clarke, M.L. & Rendelle, H.M. (2009). The impact of North Atlantic storminess on western European coasts: A review. *Quaternary International 195, 31-41.*

Clemens, S. C., & Prell, W. L. (1990). Late Pleistocene variability of Arabian Sea summer monsoon winds and continental aridity; eolian records from the lithogenic component of deep-sea sediments. *Paleoceanography, 5*(2), 109-145. doi: http://dx.doi.org/10.1029/PA005i002p00109

Dahanayake, K., & Kulasena, N. (2008). Recognition of diagnostic criteria for recent- and paleo-tsunami sediments from Sri Lanka. *Marine Geology, 254*, 3-4, 180-186. doi: http://dx.doi.org/10.1016/j.margeo.2008.06.005

DeGelleke, L., Hill, P.S., Kienast, M., Piper, D.J.W. (2013). Sediment dynamics during Heinrich event H1 inferred from grain size. *Marine Geology.* http://dx.doi.org/10.1016/j.margeo.2012.12.007.

Donat, M.G., Renggli, D., Wild, S., Alexander, L.V., Leckebusch, G.C., Ulbrich, U. (2011). Reanalysis suggests long-term upward trend in European storminess since 1871.*Geophysical Research Letters*, *38*, *14*, doi:10.1029/2011GL047995.

Dawson, A.G., Elliott, L., Mayewski, P., Lockett, P., Noone, S., Hickey, K., Holt, T., Wadhams, P., Foster, I.D.L. (2003). Late Holocene North Atlantic climate 'seesaws' and Greenland ice sheet (GISP2) paleoclimates. *The Holocene. 13, 3, 381-392.*

DeIure, A.M. (1983). *The effect of storms on sediments in Halifax Inlet, Nova Scotia*. (Unpublished Masters Thesis). Dalhousie University, Halifax, Nova Scotia.

Fader, G.B.J & Miller, R.O. (2008). Surficial geology, Halifax Harbour, Nova Scotia. *Geological Survey of Canada: Bulletin 590.*

Federici, L., & McManus, J. F. (2003). Ocean circulation and climate during the stage 11 interglacial interval. *Congress of the International Union for Quaternary Research, 16*, 138.

Fritts, H.C., Lofgren, G.R. & Gordon, G.A. (1980). Past climate reconstructed from tree rings. *Journal of Interdisciplinary History*, *4*, 773-793.

Golinski, J. (2001). Exquisite atmography: Theories of the world and experiences of the weather in diary of 1703. *British Journal of the History of Science 34, 149-171.*

Groeger, M., Henrich, R., & Bickert, T. (2003a). Glacial-interglacial variability in Lower North Atlantic Deep Water; inference from silt grain-size analysis and carbonate preservation in the Western Equatorial Atlantic. *Marine Geology, 201*(4), 321-332. doi: http://dx.doi.org/10.1016/S0025-3227(03)00263-9

Groeger, M., Henrich, R., & Bickert, T. (2003b). Variability of silt grain size and planktonic foraminiferal preservation in Plio/Pleistocene sediments from the Western Equatorial Atlantic and Caribbean. *Marine Geology, 201*(4), 307-320. doi: http://dx.doi.org/10.1016/S0025-3227(03)00264-0

Hall, I. R., McCave, I. N., Chapman, M. R., & Shackleton, N. J. (1998). Coherent deep flow variation in the Iceland and American basins during the last interglacial. *Earth and Planetary Science Letters, 164*(1-2) doi: 10.1016/S0012-821X(98)00209-X

Hansom, J.D., & Hall, A.M. (2009). Magnitude and frequency of extra-tropical North-Atlantic cyclones: A chronology from cliff-top storm deposits. *Quaternary International, 195.* doi: 10.1016/j.quaint2007.11.010.

Hays, P.D. & Grossman, E.L. (1991). Oxygen isotopes in meteoric calcite cements as indicators of continental paleoclimate. *Geology, 19, 5,* 441-444.

Henderson, G.M. (2002). New ocean proxies for paleoclimate. *Earth and Planetary Science Letters, 203,* 1-13.

Inman, D. L. (1949). Sorting of sediments in the light of fluid mechanics. *Geological Society of America Bulletin, 60*, 12.

Jouzel, J., Vimeux, F., Caillon, N., Delaygue, G., Hoffmann, G., Masson-Delmotte, V.&, Parrenin, F. (2003). Magnitude of isotope/temperature scaling for interpretation of central Antarctic ice cores. *Journal of Geophysical Research Atmospheres*. *108(D12).*

Kissel, C., Laj, C., Kienast, M., Bolliet, T., Holbourn, A., Hill, P. & Braconnot, P. (2010). Monsoon variability and deep oceanic circulation in the Western Equatorial Pacific over the last climatic cycle: Insights from sedimentary magnetic properties and sortable silt. *Paleoceanography, 25*(3), Citation PA3215. doi: http://dx.doi.org/10.1029/2010PA001980

Kontopoulos, N., & Piper, D. J. W. (1982). Storm graded sand at 200m water depth, scotian shelf, eastern canada. *Geo-Marine Letters, 2*, 1-2, 77.

Lavelle, J. W., Young, R. A., Swift, D. J. P., & Clarke, T. L. (1978). Near-bottom sediment concentration and fluid velocity-measurements on the inner continental-shelf, New-York. *Journal of Geophysical Research-Oceans and Atmospheres, 83*(NC12) doi: 10.1029/JC083iC12p06052

Ledbetter, M. T. (1986). A late pleistocene time-series of bottom-current speed in the Vema Channel. *Palaeogeography Palaeoclimatology Palaeoecology, 53*(1) doi: 10.1016/0031-0182(86)90040-4

Ma, Y., Friedrichs, C. T., Harris, K. H., & Wright, L. D. (2010). Deposition by seasonal wave and current-supported sediment gravity flows interacting with spatially varying bathymetry: Waiapu shelf, new zealand. *Marine Geology, 275*, 199.

Malaize, B., Bertran, P., Carbonel, P., Bonnissent, D., Charlier, K., Galop, D., Pujol, C. (2011). Hurricanes and climate in the Caribbean during the past 3700 years BP. *Holocene, 21*(6) doi: 10.1177/0959683611400198

Manighetti, B., & McCave, I. N. (1995). Late glacial and Holocene palaeocurrents around Rockall Bank, NE Atlantic Ocean. *Paleoceanography, 10*, 3, 611-626. doi: http://dx.doi.org/10.1029/94PA03059

Mann, M.E., Zhang, Z., Rutherford, S., Bradley, R.S., Hughes, M.K., Shindell, D., Ammann, C., Faluvegi, G. & Ni, F. (2009). Global signatures and dynamical origins of the little ice age and medieval climate anomaly. *Science. 326. 1256-1260.*

McCave , I.N. (1985). Sedimentology and stratigraphy of box cores from the Hebble site on the Nova Scotian continental rise. *Marine Geology, 66, 59-89.*

McCave, I.N. & Hall, I.R. (2006). Size sorting in marine muds: processes, pitfalls, prospects for paleoflow-speed proxies. *Geochemistry Geophysics Geosystems, 7, 10.*

McCave, I. N., Hall, I. R., & Bianchi, G. G. (2006). Laser vs. settling velocity differences in silt grainsize measurements; estimation of palaeocurrent vigour. *Sedimentology, 53*(4), 919-928. doi: http://dx.doi.org/10.1111/j.1365-3091.2006.00783.x

Mccave, I. N., Manighetti, B., & Beveridge, N. A. S. (1995b). Circulation in the glacial North-Atlantic inferred from grain-size measurements. *Nature, 374*(6518) doi: 10.1038/374149a0

McIntyre, K. L., & Howe, J. A. (2009). Bottom-current variability during the last glacial-deglacial transition, Northern Rockall Trough and Faroe Bank Channel, NE Atlantic. *Scottish Journal of Geology, 45, Part 1*, 43-57. doi: http://dx.doi.org/10.1144/0036-9276/01-375

Meeker, L.D., & Mayewski, P.A. (2002). A 1400-year high resolution record of atmospheric circulation over the North Atlantic and Asia. *The Holocene, 12, 2763-2768.*

Mortlock, R. A., & Froelich, P.N. (1989). A simple method for the rapid determination of biogenic opal in pelagic marine sediments. *Deep-Sea Res.*, *36*, 1415-1426.

Nayler, S. (2006). Nationalizing provincial weather: Meteorology in nineteenth-century Cornwall. *British Journal of the History of Science. 39, 3, 407-433.*

Nilsen, R. E. (1999). Sortable silt as a proxy for paleocurrent speed in late-Quaternary deep-sea sediments on the Vorings Plateau, Norwegian Sea. *Journal of Conference Abstracts, 4*(1), 215-216.

Noren, A. J., Bierman, P. R., Steig, E. J., Lini, A., & Southon, J. (2002). Millennial-scale storminess variability in the Northeastern United States during the Holocene Epoch. *Nature, 419*(6909) doi: 10.1038/nature01132

Nørgaard-Pedersen, N., & Mikkelsen, N. (2009). 8000 year marine record of climate variability and fjord dynamics from Southern Greenland. *Marine Geology, 264*(3–4), 177-189. doi: 10.1016/j.margeo.2009.05.004

Piper, D. J. W., Letson, J. R. J., DeIure, A. N., & Barrie, C. Q. (1983). Sediment accumulation in low-sedimentation, wave-dominated, glaciated inlets. *Sedimentary Geology, 36*, 195.

Ramirez-Herrera, M., Lagos, M., Hutchinson, I., Kostoglodov, V., Luisa Machain, M., Caballero, M., & Quintana, P. (2012). Extreme wave deposits on the Pacific Coast of Mexico: Tsunamis or storms? - A multi-proxy approach. *Geomorphology, 139*, 360-371. doi: 10.1016/j.geomorph.2011.11.002

Rodolfo, K. S., Buss, B. A., & Pilkey, O. H. (1971). Suspended sediment increase due to hurricane Gerda in continental-shelf waters off Cape Lookout, North-Carolina. *Journal of Sedimentary Petrology, 41*(4)

Shindell, D.T., Schmidt, G.A., Mann, M.E., Rind, D. & Waple, A. (2001). Solar forcing of regional climate change during the Maunder Minimum. *Science*, *294*, *2149-2152*.

Sorrel, P., Tessier, B., Demory F., Delsinne, N.,& Mouaze D. (2009). Evidence for millennial-scale climactic events in the sedimentary infilling of a macrotidal estuarine system, the Seine estuary (NW France). *Quaternary Science Reviews. 28(5-6).* doi:10.1029/2009JD012358.

Swift, D.J.P., Han, G., & Vincent, C.E. (1986). Fluid processes and sea-floor response on a modern storm-dominated shelf: Middle Atlantic Shelf of North America. Part I: The storm current regime. *CSPG Special Publications: Shelf Sands and Sandstones, Memoir 11.*

Tetra Tech EM Inc. (2003). Literature Review and Report: Surface-Sediment Sampling Technologies. Prepared for: Brian Schumacher. US Environmental Protection Agency.

Thompson, D.W.J. & Wallace, J.M. (2001). Regional climate impacts of the northern hemisphere annular mode*. Science*, 293(5527), 85-89.

Traversi, R., Usoskin, I.G., Solanki, S.K., Becagli, S., Frezzotti M., Severi, M., Stenni B. & Udisti R. (2012). Nitrate in Polar Ice: A New Tracer of Solar Variability. *Solar Physics*, 280(1), 237-254.

Trenberth K.E., Soden B., Rusticucci M., Renwick J.A., Rahimzadeh F., Parker D., Klein T.A., Easterling D., Zhai P., Jones P.D. *et al.* (2007). Observations: Surface and atmospheric climate change. *Climate Change 2007: The Physical Science Basis, Contribution of Working Group I to the Fourth Assessment Report of the Intergovernmental Panel on Climate Change.* Cambridge Univ. Press, New York. 235 – 336.

Trouet, V., Scourse, J.D. & Raible, C.C. (2012). North Atlantic storminess and Atlantic Meridonial Overturning Circulation during the last Millennium: Reconciling contradictory proxy record of NAO variability. *Global and Planetary Change 84-85. 48-55.*

Wentworth, C.R. (1922) A scale of grade and class terms for classic sediments. *Journal of Geology*. *30, 377-392*

Wheeler, D., Garcia-Herrera, R., Wilkinson, C.W. & Ward, C. (2010). Atmospheric circulation and storminess derived from Royal Navy logbooks: 1685 to 1750. *Climate Change, 101(1-2), 257-280.*

Williams, G.A. (2010). Evaluating the effects of wastewater treatment on marine sediment chemistry in Halifax Harbour, Nova Scotia. (Unpublished Masters Thesis). Dalhousie University, Halifax, Nova Scotia.

Appendix I

Methods for Coulter Counter use, Bedford Institute of Oceanography and Hill Lab, Dalhousie (Revised May 3, 2012)

Multisizer III

Current procedure for BIO and Hill Lab

Beaker = beaker or test tube with the original mud sample
Flask = round-bottom beaker (cocktail glass) used for analysis

- Ensure that all settings are appropriately entered *(refer to document MSIII Settings)*.

- Make salt water (if needed):
  - 17 g of salt;
  - 2L of Super Q (to the line);
  - Put on magnetic stirrer (cover top of flask with cup);
  - Stir until no crystal is visible;
  - Pour into filtration system.

- Pour old electrolyte into filtration system;
- Turn on filtering pump (minimum of 30 minutes);
- Turn on Multisizer III (minimum of 15 minutes);
- Open the Multisizer III program (the computer can be switched on at any time);
- Empty the waste container.

- Fill the fill/electrolyte container with salt water;
- Fill the glass container (with dispensing tube) and NaCl squirting bottle with salt water;
- Fill Super Q squirting bottles.

- To prepare samples:
  - Add salt water to sample beakers;
  - Put beakers in the sonifying bath for 10 minutes;
  - Add initial amount of sample from the beaker to a flask and record weight;
  - Rinse out small beaker with salt water to get all the particles (3 times);
  - Using salt water, dilute to ~220 ml and record exact weight;
  - Cover samples with cups when not in use;
  - Transfer label from beaker to flask.

* In prior procedures, the electrolyte used to be sonified with the Sonicator, but it is currently not done for the Multisizer III.

400 µm tube

* **Always rinse the aperture tube and the Sonicator horn between each use.**

*** Turn light off when not in use.**

- Prepare a blank.
- Set the system for the 400 tube *(do not undergo the complete procedure at this time)*:

    - Click: Run > Change Aperture Tube Wizard… ;
    - Click Next until Select the new aperture tube is highlighted;
    - Click: Aperture tube > Select the appropriate 400 tube from the list > OK;
    - Click: Close *(Change Aperture Tube Wizard window)*.
- Adjust the vacuum:
    - Click: Settings > Advanced > Sample Delivery Settings… ;
    - Set vacuum to **3.00" Hg**.
- Insert the 400 µm tube, while the vacuum regulator adjusts itself.
- Return to the Change Aperture Tube Wizard and follow the procedure *(the blank can be used when asked to insert a beaker of electrolyte)*:
    - Current: **-3200**
    - Gain: **1**
    - Measure noise level: must be under **9.58 µm** (or minimum size sampled)

* If the vacuum is adjusted prior to indicating a change of tube, the system will return the vacuum to 6.00" once the change of tube is indicated. Noise levels, however, cannot be measured prior to adjusting the vacuum, hence the importance of following the order outlined (open, close then re-open the Wizard).

- Sonify the blank for 3 minutes (with the Sonicator).

- Meanwhile, ensure that the information at the left of the screen is accurate:
    - Sample information:
        - Group ID: Core or Core_stress
        - Sample ID: Blank, Depth or Filter ID
        - Bar Code: **400**
    - SOM:
        - Time: **150** s
        - Directory: ensure that it is the appropriate one
        - File name: <G#>_<S#>_<B#>_<D>.<X>
        - Tick "Save File" (not "Include Pulse Data") and "Export Data"
        - Verify Export Directory

- Adjust size range over which data will be accumulated:
    - Click: Settings > Convert Pulses to Size Settings;
    - Enter:
        - **256** bins
        - From **9.58** µm
        - To **333** µm
    - Select:
        - Log Diameter
        - Coincidence Correction

- Run blank:
    - Insert the blank into the Multisizer III;
    - Click: Preview;
    - Ensure that the concentration is **0.0%**;
    - If needed, click: Pause > Cancel and then troubleshoot;
    - Otherwise, click: Start.

    * Sigma should be less than 600 *(from general observations)*.

- Take note of the file name *(for the blank)* and load it as background:
    - Click: Settings > Load Background Run… ;
    - Select the file name (with no #M3).

* At this point, it should be impossible to change the size range over which data is accumulated *(determined by blank)*.

- Run samples *(the background will automatically be subtracted)*:
    - Sonify with the Sonicator for 3 minutes (if filtering: sonify for 2 minutes, filter then sonify for 1 minute);

- Meanwhile, **<u>enter the appropriate Sample Information</u>** *(at the left of the screen)*;
- Set the **stirbar** and insert the sample into the Multisizer III chamber;
- Click: Preview;
- Ensure that the concentration is situated around 5% and <u>not</u> over 10% *(a little over 5% will allow for the addition of water for the following tube)*;
- If a dilution is necessary, click: Pause > Cancel;
- Otherwise, click: Start.

* When the filename appears in the graph window, the file has been saved. If the filename does not appear, manually save and export the data *(refer to document MSIII Issues and Solutions)*.

- Click: Reset *(at the left of the screen)*.

<u>200 µm tube</u>

* **<u>Always rinse the aperture tube and the Sonicator horn between each use.</u>**

*** <u>Turn light off when not in use.</u>**

- Prepare a blank.
- Set the system for the 200 tube:
  - Click: Run > Change Aperture Tube Wizard… ;
  - Click Next until Select the new aperture tube is highlighted;
  - Click: Aperture tube > Select the appropriate 200 tube from the list > OK;

* The vacuum should automatically adjust to **6.00" Hg**. If so, remain in the Change Aperture Tube Wizard. **If not, click: Close and follow the instructions to adjust the vacuum.**

- Adjust the vacuum:
  - Click: Settings > Advanced > Sample Delivery Settings… ;
  - Set vacuum to **6.00" Hg**.
- Insert the 200 µm tube, using the Change Aperture Tube Wizard:
  - Current: **-3200**
  - Gain: **1**
  - Measure noise level: <u>must</u> be under **4.17** µm (or minimum size sampled)

- Sonify the blank for 3 minutes (with the Sonicator).

- Meanwhile, ensure that the information at the left of the screen is accurate:
  - Sample information:
    - Group ID: Core or Core_stress
    - Sample ID: Blank, Depth or Filter ID
    - Bar Code: **200**
  - SOM:
    - Time: **300** s
    - Directory: ensure that it is the appropriate one
    - File name: <G#>_<S#>_<B#>_<D>_<U#>.<X>
    - Tick "Save File" (not "Include Pulse Data") and "Export Data"
    - Verify Export Directory

- Remove previous background:
  - Click: Settings > Remove Background;

- Adjust size range over which data will be accumulated:
  - Click: Settings > Convert Pulses to Size Settings;
  - Enter:
    - **256** bins
    - From **4.17** µm

        - To **145** µm
    - Select:
        - Log Diameter
        - Coincidence Correction

- Run blank:
    - Insert the blank into the Multisizer III;
    - Click: Preview;
    - Ensure that the concentration is **0.0%**;
    - If needed, click: Pause > Cancel and then troubleshoot;
    - Otherwise, click: Start;

    * A good blank should have sigma less than 1500 – 2000 after 100 s.

- Take note of the file name *(for the blank)* and load it as background:
    - Click: Settings > Load Background Run… ;
    - Select the file name (with no #M3).

* At this point, it should be impossible to change the size range over which data is accumulated *(determined by blank)*.

- Run samples *(the background will automatically be subtracted)*:
    - Sonify with the Sonicator for 3 minutes (if filtering: sonify for 2 minutes, filter then sonify for 1 minute);
    - Meanwhile, **enter the appropriate Sample Information** *(at the left of the screen)*;
    - Set the **stirbar** and insert the sample into the Multisizer III chamber;
    - Click: Preview;
    - Ensure that the concentration is situated around 5% and not over 10%;
    - If a dilution is necessary, click: Pause > Cancel;
    - Otherwise, click: Start.

    * When the filename appears in the graph window, the file has been saved. If the filename does not appear, manually save and export the data *(refer to document MSIII Issues and Solutions)*.
    - Click: Reset *(at the left of the screen)*.

30 µm tube

* **Always rinse the aperture tube and the Sonicator horn between each use.**

* **Turn light off when not in use.**

- Set the system for the 30 tube *(do not undergo the complete procedure at this time)*:
    - Click: Run > Change Aperture Tube Wizard… ;
    - Click Next until Select the new aperture tube is highlighted;
    - Click: Aperture tube > Select the appropriate 30 tube from the list > OK;
    - Click: Close *(Change Aperture Tube Wizard window)*.
- Adjust the vacuum:
    - Click: Settings > Advanced > Sample Delivery Settings… ;
    - Set vacuum to **5.00" Hg**.
- Insert the 30 µm tube, using the Change Aperture Tube Wizard again:
    - Current: **-800**
    - Gain: **4**
    - Measure noise level: must be under **0.779** µm (or minimum size sampled)

* If the vacuum is adjusted prior to indicating a change of tube, the system will return the vacuum to 6.00" once the change of tube is indicated. Noise levels, however, cannot be measured prior to adjusting the vacuum, hence the importance of following the order outlined (open, close then re-open the Wizard).

- Sonify the blank for 3 minutes (with the Sonicator);
- Meanwhile, ensure that the information at the left of the screen is accurate:
    - Sample information:
        - Group ID: Core or Core_stress
        - Sample ID: Blank, Depth or Filter ID
        - Bar Code: **30**
    - SOM:
        - Time: **250** s
        - Directory: ensure that it is the appropriate one
        - File name: <G#>_<S#>_<B#>_<D>_<U#>.<X>
        - Tick "Save File" (not "Include Pulse Data") and "Export Data"
        - Verify Export Directory

- Remove previous background:
    - Click: Settings > Remove Background;

- Adjust size range over which data will be accumulated:
    - Click: Settings > Convert Pulses to Size Settings;
    - Enter:
        - **256** bins
        - From **0.779** µm
        - To **27.1** µm
    - Select:
        - Log Diameter
        - Coincidence Correction
- Run blank:
    - Insert the blank into the Multisizer III;
    - Click: Preview;
    - Ensure that the concentration is **0.0%**;
    - If needed, click: Pause > Cancel and then troubleshoot;
    - Otherwise, click: Start.
        * A good blank should have sigma less than 7500 after 100 s.

- Take note of the file name *(for the blank)* and load it as background:
    - Click: Settings > Load Background Run… ;
    - Select the file name (with no #M3).

* At this point, it should be impossible to change the size range over which data is accumulated *(determined by blank)*.

- Run samples *(the background will automatically be subtracted)*:
    - Sonify with the Sonicator for 3 minutes (if filtering: sonify for 2 minutes, filter then sonify for 1 minute);
    - Meanwhile, **<u>enter the appropriate Sample Information</u>** *(at the left of the screen)*;
    - Pour some of the sample into a small beaker;
    - Insert the beaker into the Multisizer III chamber (**no stirbar**);
    - **<u>Adjust the aperture view in order to see the aperture</u>**;
    - Click: Preview;
    - Ensure that the concentration is situated around 5% and <u>not over 10%</u>;
    - If a dilution is necessary, click: Pause > Cancel;
    - Otherwise, click: Start.
    * When the filename appears in the graph window, the file has been saved. If the filename does not appear, manually save and export the data *(refer to document MSIII Issues and Solutions)*.

    - Click: Reset *(at the left of the screen)*.

* The 30 µm tube may require additional sonication and filtering. Simply persevere until the aperture does not clog.

Appendix II

Matlab Code for Merging Output Distributions from the Multisizer III Coulter Counter: Written by John Newgard (Dalhousie University)

```
% MERGEPROCESSOR    Merges Multisizer III size
distributions.
% The merge processor requires the user to manually
enter the sample name
%(e.g. 'ME24_347', including the quotes) at the
prompt. To process many
%   samples, use MERGEPROCESSOR_BATCH.
%   Sample data must be in .CSV (or .csv) format.
%   This script was written to process Multisizer
data from 30-, 200-, and
%   400-micron aperture tubes.  To alter this,
change the value of the
%   variable TUBE_SIZES (and possibly the plotting
axis limits).
%   SET-UP INSTRUCTIONS:
%   1. Folders should be set-up as follows:
%       - Root Directory (see next instruction)
%           - MergedData
%               - figures
%           - ToMergeProcessor
%           - matlab (recommended, but not
necessary)
%           - RawData (recommended, but not
necessary)
%   2. Ensure that the MergeProcessor.m, MU2PHI.M,
and
%   MULTISIZER_MERGEBINS_30_200_400.M files are
either in the same
%   directory or that the two directories are both
in Matlab's search path
%   (File > Set Path).
%   3. Specify your root directory name by changing
the variable 'dir_root'
%   (below); e.g. dir_root =
'C:\Work\Project\Merging\';
%   4. Put data files in the TOMERGEPROCESSOR
folder.
%   5. Ensuring that you are in the same directory
as the MERGEPROCESSOR.M
%  file, type 'MergeProcessor' or
'MergeProcessor_batch' at the prompt.
%  If you wish to stray from the recommended
directory structure, you will
%   need to replace the values of all 'dir_XXXX'
variables in the code.
%   Code not working for you?  Send me an email and
complain!
%   MULTISIZER OUTPUT FORMAT:
%       data begins on line 30 (29 lines of header)
%       Col 1. bin number
%       Col 2. lower bin diameter (microns)
%       Col 3. center bin diameter (microns)
%       Col 4. particle count
%       Col 5. normalized volume concentration (%)
%   Recent Changes:
```

```
%       June:
%       You can choose to process data from either
two or three tubes.
%       Can now handle data files that include
headers.
%       Removes the .#M3 from filenames
%       July:
%       Figure positioning has been improved using
normalization
% By John Newgard, July 2010.
john_newgard@hotmail.com
addpath('/Users/erinwilson/Desktop/DalhousieOceanog
raphy/MatlabFunctions/');
warning off
clear
close all

dir_root =
'/Users/erinwilson/Desktop/DalhousieOceanography/Mu
ltisizer_III/';
dir_data = [dir_root 'ToMergeProcessor/'];
dir_merged = [dir_root 'MergedData/'];
dir_fig = [dir_merged 'figures/'];

image_ext_1 = '.CSV';
image_ext_2 = '.csv';
tube_sizes_all = [30 200 400];

%% Set figure properties using NORMALIZED UNITS
% Determine Screen Size Variable 3=Width 4=Height
set(0,'Units','normalized');
% We want the first figure, used for merging, to be
1/2 height and centered.
% We want the others to be 1/2 of the screen width
and height
FIGURE_WIDTH = .49;
FIGURE_HEIGHT = .5;

% Set the position for each figure
FIGURE_1_COORDINATES = [.25 .5 FIGURE_WIDTH
FIGURE_HEIGHT];
FIGURE_2_COORDINATES = [.005 .5 FIGURE_WIDTH
FIGURE_HEIGHT];
FIGURE_3_COORDINATES = [.505 .5 FIGURE_WIDTH
FIGURE_HEIGHT];


%% Get directory listing
dir_wkg = pwd;
eval(['cd ' dir_data])
eval(['!ls *_' num2str(tube_sizes_all(1)) '*'
image_ext_1 ' > list1_temp.txt'])
eval(['!ls *_' num2str(tube_sizes_all(1)) '*'
image_ext_2 ' > list2_temp.txt'])
eval(['cd ' dir_wkg])
fnames = rd_list([dir_data 'list1_temp.txt']);
fnames = [fnames rd_list([dir_data
'list2_temp.txt'])];

for ia = 1:length(fnames)
    I = find((fnames{ia}=='_')==1);
    tempchar = fnames{ia};
    samplenames{ia} = tempchar(1:I(2)-1); % e.g. =
'ME24_347'
end

tube_sizes_all = [30 200 400];

%% MAIN LOOP
for ia = 1:length(samplenames) % For each set of
samples...
    samplename = samplenames{ia};

    eval(['cd ' dir_data])
    eval(['!ls *' samplename '*.* >
list_temp.txt'])
```

```
eval(['cd ' dir_wkg])
    fnames = rd_list([dir_data 'list_temp.txt']);

    ntubes = length(fnames);
    if ntubes == 2
        tube_sizes = tube_sizes_all(1:2);
        %tube_str = [num2str(tube_sizes(1)) '_'
num2str(tube_sizes(2))];
    elseif ntubes == 3
        %tube_str = [num2str(tube_sizes(1)) '_'
num2str(tube_sizes(2)) '_' num2str(tube_sizes(3))];
        tube_sizes = tube_sizes_all;
    end

    fname_char = fnames{1}; % e.g.
ME24_347_200_2010-02-01.#M3.CSV
    temp = fname_char(length(samplename)+1:end-4);
    I = find(temp=='#');
    I2 = find(temp=='_');
    if isfinite(I)
        suffix = temp(I2(2):I-2);
    else
        suffix = temp(I2(2):end);
    end
    eval(['exportname = ''' samplename suffix
'_merged'';']); % e.g. 'ME24_347_2010-02-01_merged'


    ntubes = length(tube_sizes);


    %% Create input filename syntax
    fname_raw1 = fnames{2}; % e.g.
ME24_347_30_2010-02-01.CSV
    fname_raw2 = fnames{1}; % e.g.
ME24_347_200_2010-02-01.CSV
    if ntubes==3
        fname_raw3 = fnames{3}; % e.g.
ME24_347_400_2010-02-01.CSV
    end
    %% Read the data files and assign data to
variables listed on left below
    fid = fopen([dir_data fname_raw1]);
    C =
textscan(fid,'%u%f%f%u%f','Delimiter',',','HeaderLi
nes',29);
    fclose(fid);
    I = find(C{1}~=0);
    bnum1 = C{1}; bnum1 = bnum1(I);
    lowd1 = C{2}; lowd1 = lowd1(I);
    centd1 = C{3}; centd1 = centd1(I);
    count1 = C{4}; count1 = count1(I);
    dvol1 = C{5}; dvol1 = dvol1(I);

    fid = fopen([dir_data fname_raw2]);
    C =
textscan(fid,'%u%f%f%u%f','Delimiter',',','HeaderLi
nes',29);
    fclose(fid);
    I = find(C{1}~=0);
    bnum2 = C{1}; bnum2 = bnum2(I);
    lowd2 = C{2}; lowd2 = lowd2(I);
    centd2 = C{3}; centd2 = centd2(I);
    count2 = C{4}; count2 = count2(I);
    dvol2 = C{5}; dvol2 = dvol2(I);
if ntubes==3
        fid = fopen([dir_data fname_raw3]);
        C =
textscan(fid,'%u%f%f%u%f','Delimiter',',','HeaderLi
nes',29);
        fclose(fid);
        I = find(C{1}~=0);
        bnum3 = C{1}; bnum3 = bnum3(I);
        lowd3 = C{2}; lowd3 = lowd3(I);
        centd3 = C{3}; centd3 = centd3(I);
        count3 = C{4}; count3 = count3(I);
```

```
        dvol3 = C{5}; dvol3 = dvol3(I);
    end
    %% Sort the binned data by tube diameter
    temp = [centd1(1) centd2(1)];
    if ntubes==3
        temp = [temp centd3(1)];
    end
    [junk I] = sort(temp,'ascend');
    if ntubes==3
        eval(['centd_mu = [centd' num2str(I(1)) '
centd' num2str(I(2)) ' centd' num2str(I(3)) '];'])
        eval(['lowd_mu = [lowd' num2str(I(1)) '
lowd' num2str(I(2)) ' lowd' num2str(I(3)) '];'])
        centd_phi = mu2phi(centd_mu);
        lowd_phi = mu2phi(lowd_mu);
        eval(['dvol = [dvol' num2str(I(1)) ' dvol'
num2str(I(2)) ' dvol' num2str(I(3)) '];'])
        eval(['numparticles = [count' num2str(I(1))
' count' num2str(I(2)) ' count' num2str(I(3))
'];'])
    else
        eval(['centd_mu = [centd' num2str(I(1)) '
centd' num2str(I(2)) '];'])
        eval(['lowd_mu = [lowd' num2str(I(1)) '
lowd' num2str(I(2)) '];'])
        centd_phi = mu2phi(centd_mu);
        lowd_phi = mu2phi(lowd_mu);
        eval(['dvol = [dvol' num2str(I(1)) ' dvol'
num2str(I(2)) '];'])
        eval(['numparticles = [count' num2str(I(1))
' count' num2str(I(2)) '];'])
    end


    % Get merge bins
    centd_mu_new = multisizer_mergebins_30_200_400;
    %eval(['[centd_mu_new,lowerd_mu,upperd_mu] =
multisizer_mergebins_' tube_str ';'])
    %eval(['centd_mu_new = multisizer_mergebins_'
tube_str ';'])
    % Get the volumes and counts that correspond to
the merge bins.
    %   - merged volumes correpond to the sum of
the volumes in the 10
    %       consecutive bins centered about the
merge bins
    %   - if there are less than 5 diameter bins on
either side of the
    %       merge bin centre, the volume for that
merged bin is given a
    %     value of NaN and the particle count is
given a value of zero.
    phi = mu2phi(centd_mu_new);
    for ii = 1:ntubes
        diam = centd_phi(:,ii);
        vol = dvol(:,ii);
        num = numparticles(:,ii);
        for jj = 1:length(phi)
            [y I] = min(abs(phi(jj) - diam));
            if diam(I) < phi(jj)
                if I-4>0 & I+5<=length(diam)
                    dvol_new(jj,ii) = sum(vol(I-
4:I+5));
                    numparticles_new(jj,ii) =
sum(num(I-4:I+5));
                else
                    dvol_new(jj,ii) = NaN;
                    numparticles_new(jj,ii) = NaN;
                end
            else
                if I-5>0 & I+4<length(diam)
                    dvol_new(jj,ii) = sum(vol(I-
5:I+4));
                    numparticles_new(jj,ii) =
sum(num(I-5:I+4));
                else
```

```
                    dvol_new(jj,ii) = NaN;
                    numparticles_new(jj,ii) = NaN;
                end
            end
        end
    end


    % Remove spurious points with <10 counts/bin at
large-diameter end of
    % each distribution.  NB. Data in diameter bins
>= the smallest of
    % these bins will ALL be removed.
    for ii = 1:ntubes
        % First replace zero values with NaNs
        I = find(numparticles_new(:,ii)==0);
        numparticles_new(I,ii) = NaN;
        dvol_new(I,ii) = NaN;
        % Now find counts less than 10
        I = find(numparticles_new(:,ii)<10);
        if isfinite(I)
            I_good = [1:min(I)-1]';
        else
            I_good =
[1:length(numparticles_new(:,ii))];
        end
        I_bad =
find(ismember([1:length(numparticles_new)],I_good)=
=0);
        numparticles_new(I_bad,ii) = NaN;
        dvol_new(I_bad,ii) = NaN;
    end

    % Remove NaN values from distributions
    I = find(isfinite(numparticles_new(:,1))==1);
    dvol1 = dvol_new(I,1);
    centd_mu_1 = centd_mu_new(I);
    %lowerd_mu_1 = lowerd_mu(I);
    %upperd_mu_1 = upperd_mu(I);
    I = find(isfinite(numparticles_new(:,2))==1);
    dvol2 = dvol_new(I,2);
    centd_mu_2 = centd_mu_new(I);
    %lowerd_mu_2 = lowerd_mu(I);
    %upperd_mu_2 = upperd_mu(I);
    if ntubes==3
        I =
find(isfinite(numparticles_new(:,3))==1);
        dvol3 = dvol_new(I,3);
centd_mu_3 = centd_mu_new(I);
        %lowerd_mu_3 = lowerd_mu(I);
        %upperd_mu_3 = upperd_mu(I);
    end
    centd1 = centd_mu_1;
    centd2 = centd_mu_2;
    if ntubes==3
        centd3 = centd_mu_3;
    end
    % Set axis limits for figures
    xmin = 1; xmax = 1000;
    ymin = .1; ymax = 100;
    mergeok = 0;
    while mergeok == 0;
        % plot unmerged curves to determine
diameters for merging
        figure(1), clf

set(gcf,'Units','normalized','OuterPosition',FIGURE
_1_COORDINATES);
        loglog(centd1,dvol1,'.-r'), hold on
        loglog(centd2,dvol2,'.-b')
        if ntubes==3
            loglog(centd3,dvol3,'.-g')
        end
        xlabel('Diameter (\mum)','fontsize',14)
        ylabel('Normalized Vol. Conc.
(%)','fontsize',14)
```

```
        axis([xmin xmax ymin ymax])
        axis square
        %% Find bins associated with merging
diameters
        if ntubes==3
            title([samplename '    Click figure,
then click on two suitable merge points, then hit
ENTER'],'Interpreter','none','FontSize',14)
            disp('')
            disp('USER INPUT REQUIRED:');
            disp('')
            disp('  Use the crosshairs to select
the x-values at which you want ');
            disp('   the red/blue, and blue/green,
curves to be merged.');
            disp('')
            disp('  1. Line-up the vertical line
(horiz line does not matter) where you want it.');
            disp('  2. Click the mouse.');
            disp('  3. Move to the 2nd merge point
and click.');
            disp('  4. Hit ENTER.');
        else
            title([samplename '   Click figure,
then click on a suitable merge point, then hit
ENTER'],'Interpreter','none','FontSize',14)
            disp('')
            disp('USER INPUT REQUIRED:');
            disp('  Use the crosshairs to select
the x-value at which you want ');
            disp('   the red and blue curves to be
merged.');
            disp('')
            disp('  1. Line-up the vertical line
(horiz line does not matter) where you want it.');
            disp('  2. Click the mouse.');
            disp('  3. Hit ENTER.');
        end
        % Find the indices of the merge bins
        % Dist'ns 1 & 2
        [mergepts,junk] = ginput; % puts cross-
hairs on the figure and saves the points
        if size(mergepts)~=ntubes-1
            close
            if ntubes==3
                disp('You must click on the figure
TWICE.  Please re-try.')
            else
                disp('It did not work.  Try again.
Make sure you have activated the figure, by
clicking on it, before you click to select your
points.')
            end
            pause(3); % This pauses for 3 seconds
        else
            j1 = max(find(centd1<=mergepts(1)));
            k1 = min(find(centd2>=mergepts(1)));
            % Dist'ns 2 & 3
            if ntubes==3
                j2 =
max(find(centd2<=mergepts(2)));
                k2 =
min(find(centd3>=mergepts(2)));
            end
            % Close the figure
            close

            %%      New merging scheme
            % 1. Scale the smallest-aperture curve
to meet the middle curve and truncate it up to
            % the merge point.
            beta1 = dvol2(k1)/dvol1(j1);
            merge_dvol1 = beta1.*dvol1(1:j1);
            merge_centd1 = centd1(1:j1);

            if ntubes==3
```

```
                % 2. Scale the largest-aperture
curve to meet the middle curve and truncate it up
to
                % the merge point.
                beta2 = dvol2(j2)/dvol3(k2);
                merge_dvol3 = beta2.*dvol3(k2:end);
                merge_centd3 = centd3(k2:end);
            else
                beta2 = [];
                merge_dvol3 = [];
                merge_centd3 = [];
            end

            if ntubes==3
                % 3. Truncate the middle curve
between the merge points.
                merge_dvol2 = dvol2(k1:j2);
                merge_centd2 = centd2(k1:j2);
            else
                merge_dvol2 = dvol2(k1:end);
                merge_centd2 = centd2(k1:end);
            end
            % 4. Merge these truncated curves
            merge_dvol = [merge_dvol1; merge_dvol2;
merge_dvol3];
            merge_centd = [merge_centd1;
merge_centd2; merge_centd3];

            % Plot the merged curve with the
unmerged curves
            %         xmin = min(centd1) -
0.5*min(centd1);
            %         xmax = max(centd3) +
max(centd3);
            %         ymin = min([min(merge_dvol)
min(dvol3)]) - 0.5*min([min(merge_dvol)
min(dvol3)]);
            %         ymax = max([dvol1; dvol2;
dvol3; merge_dvol]) + max([dvol1; dvol2; dvol3;
merge_dvol]);
            xmin = 1; xmax = 1000; ymin = .1; ymax
= 100;
            figure(2), clf

set(gcf,'Units','normalized','OuterPosition',FIGURE
_2_COORDINATES);
            loglog(merge_centd,merge_dvol,'-
k','LineWidth',2), hold on
            loglog(centd1,dvol1,'-r','LineWidth',1)
            loglog(centd2,dvol2,'-b','LineWidth',1)
            if ntubes==3
                loglog(centd3,dvol3,'-
g','LineWidth',1)
            end
            loglog([mergepts(1) mergepts(1)],[ymin
ymax],'-.','Color',[.7 .7 .7])
            if ntubes==3
                loglog([mergepts(2)
mergepts(2)],[ymin ymax],'-.','Color',[.7 .7 .7])
            end
            axis([xmin xmax ymin ymax])
            axis square
            xlabel('Diameter (\mum)','fontsize',14)
            ylabel('Normalized Vol. Conc.
(%)','fontsize',14)
            if ntubes==3

AX=legend('merged',[num2str(tube_sizes(1)) '
\mum'],[num2str(tube_sizes(2)) ' \mum']...
                        ,[num2str(tube_sizes(3)) '
\mum']);
            else

AX=legend('merged',[num2str(tube_sizes(1)) '
\mum'],[num2str(tube_sizes(2)) ' \mum']);
            end
```

```
set(AX,'FontSize',8,'Location','north'), legend
boxoff
            title('Accept or reject the merged
curve?')
            %% Normalize the merged distribution
            sumpercentages = sum(merge_dvol);
            merge_dvol_norm =
merge_dvol./sumpercentages.*100;
            figure(3), clf

set(gcf,'Units','normalized','OuterPosition',FIGURE
_3_COORDINATES);
            loglog(merge_centd,merge_dvol_norm,'-
k','LineWidth',2), hold on
            loglog([mergepts(1) mergepts(1)],[ymin
ymax],'-.','Color',[.7 .7 .7])
            if ntubes==3
                loglog([mergepts(2)
mergepts(2)],[ymin ymax],'-.','Color',[.7 .7 .7])
            end
            axis([xmin xmax ymin ymax])
            xlabel('Diameter (\mum)','fontsize',14)
            ylabel('Normalized Vol. Conc.
(%)','fontsize',14)
            title('Accept or reject the merged
curve?')
            axis square
            if min(merge_dvol_norm) < 0.1
                axis([xmin xmax .01 ymax])
                set(gca,'PlotBoxAspectRatio',[3 4
1])
            end
            answerok = 0;
            while answerok == 0;
                yesorno = input('Do you accept this
merged curve (y/n)? [y]','s');
                if isempty(yesorno) |
strcmp(yesorno,'y') | strcmp(yesorno,'yes') |
strcmp(yesorno,'Y') | strcmp(yesorno,'Yes') |
strcmp(yesorno,'YES')
                    mergeok = 1; answerok = 1;
                elseif strcmp(yesorno,'n') |
strcmp(yesorno,'no') | strcmp(yesorno,'No') |
strcmp(yesorno,'NO') | strcmp(yesorno,'N')
                    mergeok = 0; answerok = 1;
                else disp(['Your answer was not
understood.  Please type ''y'' or ''n''.'])
                    answerok = 0;
                end
            end
            figure(2), close
            figure(3)
            % Save the figure to a jpeg file
            title(samplename,'Interpreter','none')
            print('-djpeg100','-r200',[dir_fig
exportname '.jpg'])
        end

    end
    %% OUTPUT THE MERGED DISTRIBUTIO
    merge_dvol = merge_dvol_norm;
    % Save text file
    data_out = [merge_centd merge_dvol];
    dlmwrite([dir_merged exportname
'.csv'],data_out,',')
    %edit([dir_merged exportname '.csv']) % This
opens the output text
    % file in the matlab editor
    % Save .mat file
    eval(['save ' dir_merged exportname '.mat
merge_centd merge_dvol'])
end
```

Appendix III

Figures for Other Metrics Measured

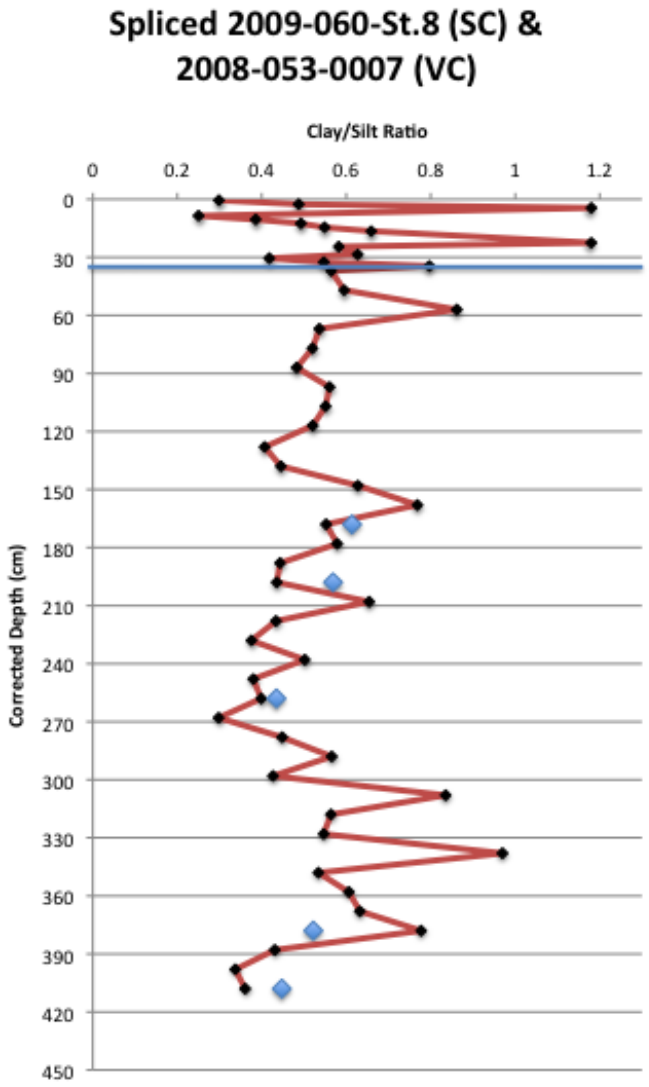

Figure AIII.1: Clay/silt ratio versus depth (corrected) in the spliced record from the Northwest Arm. Blue line indicates where the cores were spliced. Blue diamonds show duplicate runs.

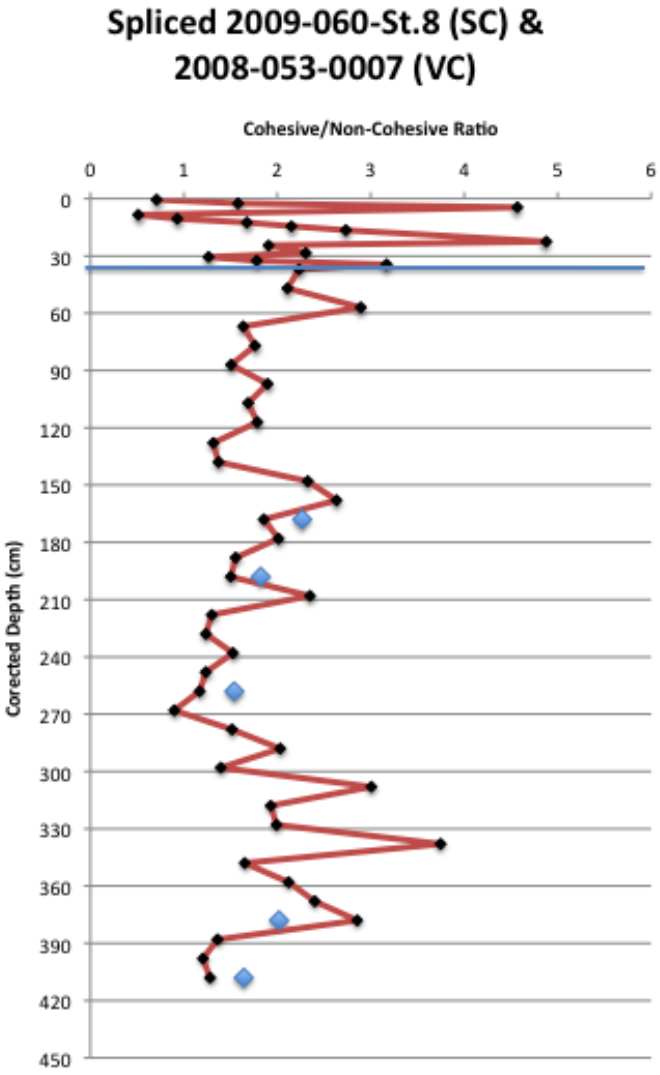

Figure AIII.2: Cohesive/non-Cohesive ratio versus depth (corrected) in the spliced record from the Northwest Arm. Blue line indicates where the cores were spliced. Blue diamonds show duplicate runs.

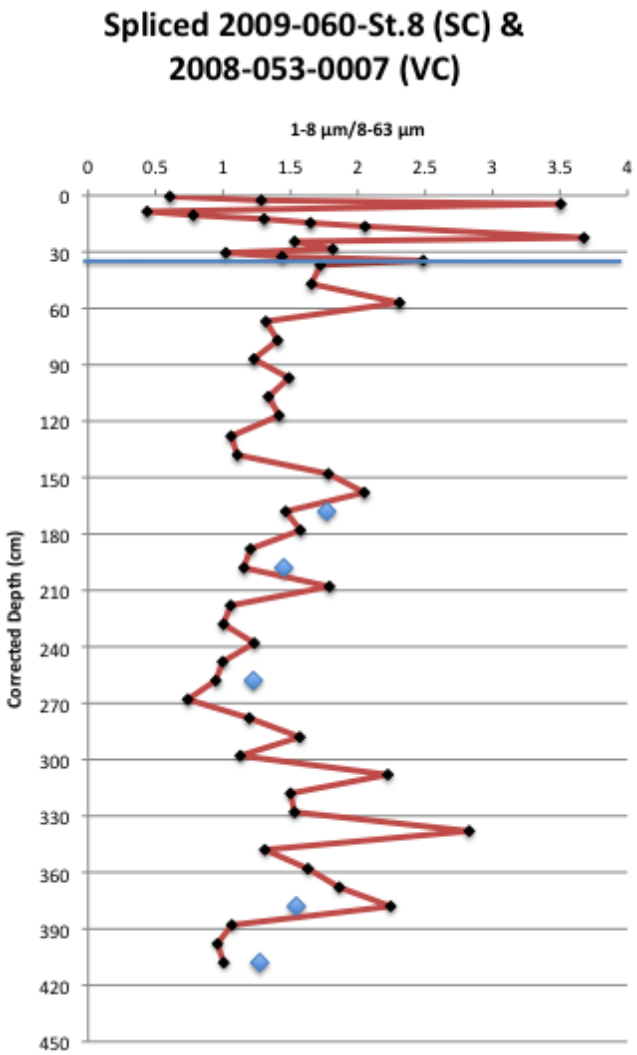

Figure AIII.3: 1-8 µm/8-63 µm ratio versus depth (corrected) in the spliced record from the Northwest Arm. Blue line indicates where the cores were spliced. Blue diamonds show duplicate runs.

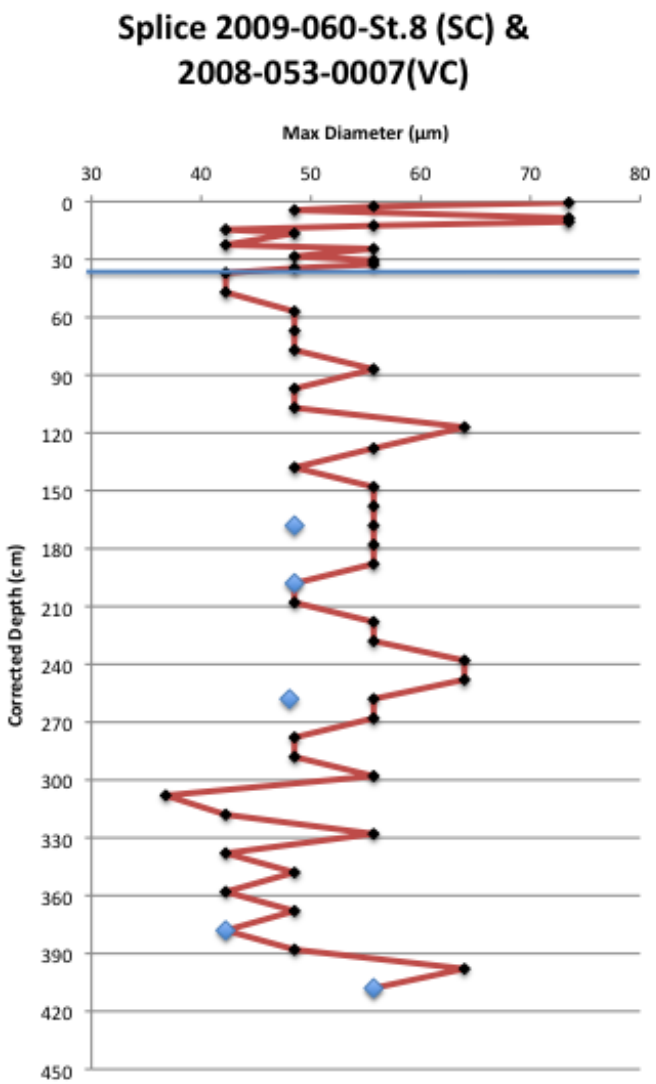

Figure AIII.4: Maximum diameter versus depth (corrected) in the spliced record from the Northwest Arm. Blue line indicates where the cores were spliced. Blue diamonds show duplicate runs.

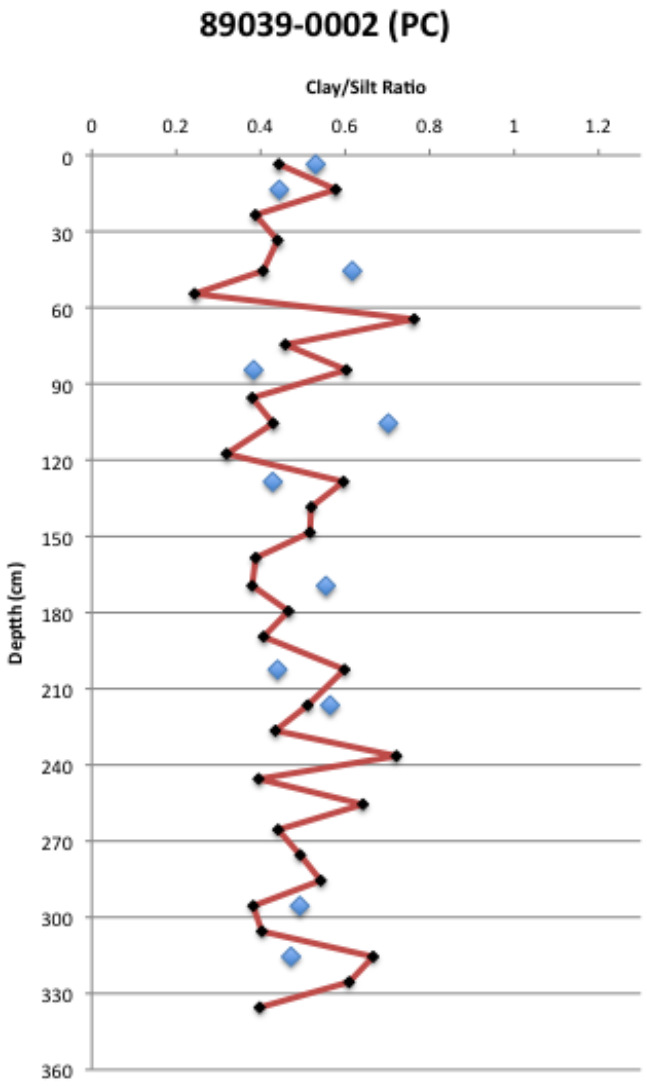

Figure AIII.5: Clay/Silt ratio versus depth in core 89039-0002 from Purcell's Cove. Blue diamonds show duplicate runs.

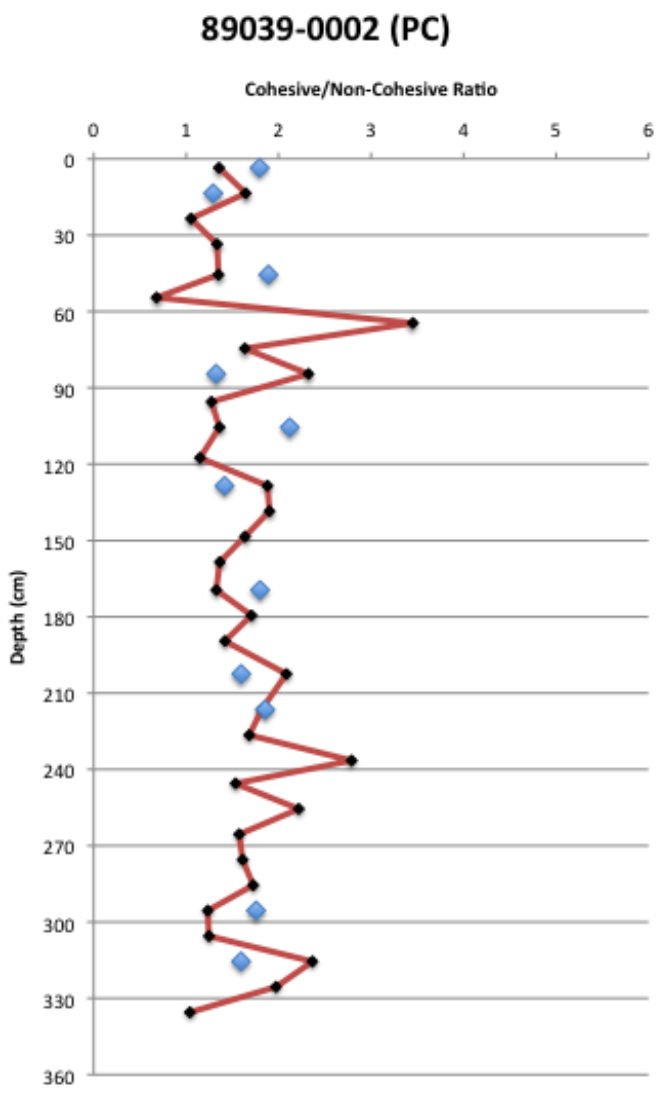

Figure AIII.6: Cohesive/non-cohesive ratio versus depth in core 89039-0002 from Purcell's Cove. Blue diamonds show duplicate runs.

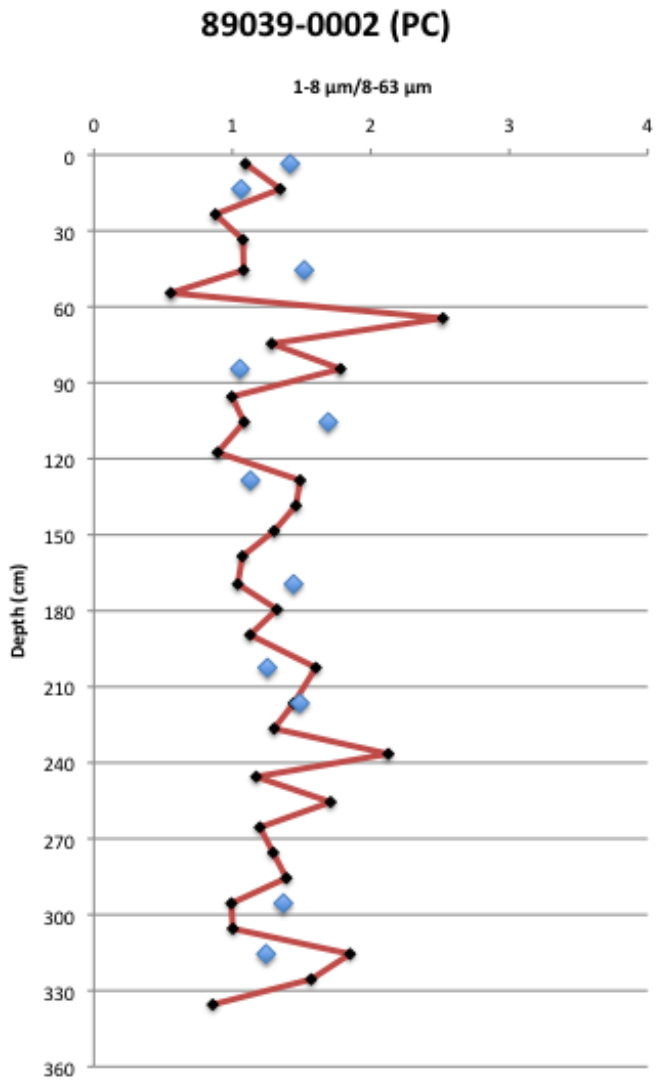

Figure AIII.7: 1-8 µm/1-63 µm ratio versus depth in core 89039-0002 from Purcell's Cove. Blue diamonds show duplicate runs.

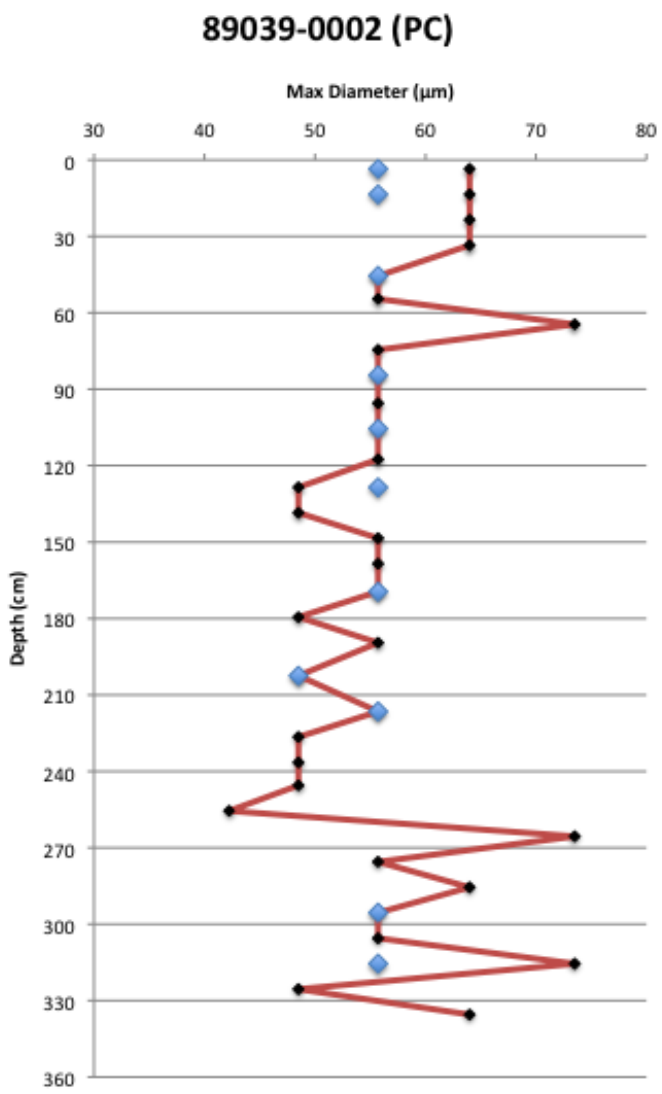

Figure AIII.8: Maximum diameter versus depth in core 89039-0002 from Purcell's Cove. Blue diamonds show duplicate runs.

Appendix IV

Core Data

Northwest Arm : Spliced Core

Original Core	Sample Depth (cm)	Corrected Depth	Age (.2cm/yr)	SS	Clay/Silt Ratio	Cohesive/Non Cohesive Ratio	1-8 µm/8-63 µm Ratio
Slow Core	0.5	0.5	2.5	26.9	0.3	0.7	0.6
Slow Core	2.5	2.5	12.5	19.3	0.5	1.6	1.3
Slow Core	4.5	4.5	22.5	16.5	1.2	4.6	3.5
Slow Core	8.5	8.5	42.5	25.2	0.3	0.5	0.4
Slow Core	10.5	10.5	52.5	24.8	0.4	0.9	0.8
Slow Core	12.5	12.5	62.5	17.6	0.5	1.7	1.3
Slow Core	14.5	14.5	72.5	16.3	0.5	2.2	1.6
Slow Core	16.5	16.5	82.5	15.7	0.7	2.7	2.1
Slow Core	22.5	22.5	112.5	15.1	1.2	4.9	3.7
Slow Core	24.5	24.5	122.5	18.6	0.6	1.9	1.5
Slow Core	28.5	28.5	142.5	17.5	0.6	2.3	1.8
Slow Core	30.5	30.5	152.5	19.5	0.4	1.3	1.0
Slow Core	32.5	32.5	162.5	18.9	0.5	1.8	1.4
Slow Core	34.5	34.5	172.5	16.0	0.8	3.2	2.5
Vibra Core	21.5	37	185	15.6	0.6	2.2	1.7
Vibra Core	31.5	47	235	16.5	0.6	2.1	1.7
Vibra Core	41.5	57	285	17.7	0.9	2.9	2.3
Vibra Core	51.5	67	335	18.3	0.5	1.6	1.3
Vibra Core	61.5	77	385	17.7	0.5	1.8	1.4
Vibra Core	71.5	87	435	20.0	0.5	1.5	1.2
Vibra Core	81.5	97	485	17.3	0.6	1.9	1.5
Vibra Core	91.5	107	535	17.1	0.6	1.7	1.3
Vibra Core	101.5	117	585	17.9	0.5	1.8	1.4
Vibra Core	112.5	128	640	19.0	0.4	1.3	1.1
Vibra Core	122.5	138	690	18.8	0.4	1.4	1.1
Vibra Core	132.5	148	740	17.0	0.6	2.3	1.8
Vibra Core	142.5	158	790	17.2	0.8	2.6	2.0
Vibra Core	152.5	168	840	17.4	0.6	1.9	1.5
Vibra Core	162.5	178	890	17.4	0.6	2.0	1.6

Vibra Core	172.5	188	940	18.0	0.4	1.6	1.2
Vibra Core	182.5	198	990	17.0	0.4	1.5	1.2
Vibra Core	192.5	208	1040	15.8	0.7	2.3	1.8
Vibra Core	202.5	218	1090	19.9	0.4	1.3	1.1
Vibra Core	212.5	228	1140	20.1	0.4	1.2	1.0
Vibra Core	222.5	238	1190	19.8	0.5	1.5	1.2
Vibra Core	232.5	248	1240	21.2	0.4	1.2	1.0
Vibra Core	242.5	258	1290	19.5	0.4	1.2	0.9
Vibra Core	252.5	268	1340	21.0	0.3	0.9	0.7
Vibra Core	262.5	278	1390	17.5	0.4	1.5	1.2
Vibra Core	272.5	288	1440	16.9	0.6	2.0	1.6
Vibra Core	282.5	298	1490	18.9	0.4	1.4	1.1
Vibra Core	292.5	308	1540	14.6	0.8	3.0	2.2
Vibra Core	302.5	318	1590	16.9	0.6	1.9	1.5
Vibra Core	312.5	328	1640	16.5	0.5	2.0	1.5
Vibra Core	322.5	338	1690	14.8	1.0	3.7	2.8
Vibra Core	332.5	348	1740	18.1	0.5	1.7	1.3
Vibra Core	342.5	358	1790	15.9	0.6	2.1	1.6
Vibra Core	352.5	368	1840	16.7	0.6	2.4	1.9
Vibra Core	362.5	378	1890	17.0	0.8	2.9	2.2
Vibra Core	372.5	388	1940	17.8	0.4	1.4	1.1
Vibra Core	382.5	398	1990	18.8	0.3	1.2	1.0
Vibra Core	392.5	408	2040	19.2	0.4	1.3	1.0

Purcell's Cove: Piston Core

Sample Depth (cm)	Depth + 20cm	Age	SS	Clay/Silt Ratio	Cohesive/Non Cohesive Ratio	1-8 µm/8-63 µm Ratio
3.5	23.5	117.5	21.3	0.4	1.4	1.1
13.5	33.5	167.5	20.4	0.6	1.6	1.3
23.5	43.5	217.5	22.9	0.4	1.1	0.9
33.5	53.5	267.5	21.3	0.4	1.3	1.1
45.5	65.5	327.5	20.5	0.4	1.3	1.1
54.5	74.5	372.5	22.1	0.2	0.7	0.6
64.5	84.5	422.5	19.1	0.8	3.5	2.5
74.5	94.5	472.5	18.5	0.5	1.6	1.3
84.5	104.5	522.5	17.7	0.6	2.3	1.8
95.5	115.5	577.5	20.5	0.4	1.3	1.0
105.5	125.5	627.5	19.4	0.4	1.4	1.1
117.5	137.5	687.5	18.7	0.3	1.2	0.9
128.5	148.5	742.5	17.4	0.6	1.9	1.5
138.5	158.5	792.5	17.1	0.5	1.9	1.5
148.5	168.5	842.5	18.6	0.5	1.6	1.3
158.5	178.5	892.5	18.4	0.4	1.4	1.1
169.5	189.5	947.5	18.7	0.4	1.3	1.0
179.5	199.5	997.5	17.4	0.5	1.7	1.3
189.5	209.5	1047.5	17.9	0.4	1.4	1.1
202.5	222.5	1112.5	16.5	0.6	2.1	1.6
216.5	236.5	1182.5	18.9	0.5	1.8	1.4
226.5	246.5	1232.5	17.1	0.4	1.7	1.3
236.5	256.5	1282.5	16.4	0.7	2.8	2.1
245.5	265.5	1327.5	17.2	0.4	1.5	1.2
255.5	275.5	1377.5	16.3	0.6	2.2	1.7
265.5	285.5	1427.5	17.8	0.4	1.6	1.2
275.5	295.5	1477.5	18.6	0.5	1.6	1.3
285.5	305.5	1527.5	19.8	0.5	1.7	1.4
295.5	315.5	1577.5	18.8	0.4	1.2	1.0
305.5	325.5	1627.5	19.5	0.4	1.2	1.0
315.5	335.5	1677.5	19.0	0.7	2.4	1.9
325.5	345.5	1727.5	17.6	0.6	2.0	1.6
335.5	355.5	1777.5	21.7	0.4	1.0	0.9